Nonlinear Directional Fiber Couplers in Optical Communication Systems: A Performance Analysis

by

M.Sc. Néstor Lozano Crisóstomo
INAOE

Thesis submitted as partial requirement for the degree of

DOCTOR IN SCIENCES WITH SPECIALITY OF OPTICS

at

Instituto Nacional de Astrofísica Óptica y Electrónica
Santa Maria Tonantzintla, Puebla.

Supervised by:

Dr. José Javier Sánchez Mondragón
INAOE

Prof. Govind P. Agrawal
University of Rochester

and

Dr. Daniel Alberto May Arrioja
CIO

Nonlinear Directional Fiber Couplers in Optical Communication Systems: A Performance Analysis

Submitted by

M. Sc. Néstor Lozano Crisóstomo

Dissertation Submitted in Partial Fulfilment of the Requirements for the Degree of Doctor of Philosophy in Optical Sciences

Supervised by

Dr. José Javier Sánchez Mondragón
INAOE

Prof. Govind P. Agrawal
University of Rochester

and

Dr. Daniel Alberto May Arrioja
CIO

Optics Department
Instituto Nacional de Astrofísica, Óptica y Electrónica
Santa María Tonantzintla, Puebla, México

December 2015

To my grandparents Isidora and Juan.

To Nataly and Néstor

And to my mother Maria Luisa

Acknowledgements

This dissertation would not have been possible without the guidance and help of several individuals who in one way or another contributed and extended their valuable assistance in the preparation and completion of this study. First and foremost, I am heartily thankful to my advisor and friend, Dr. José Javier Sánchez Mondragón for his invaluable support, advice, recommendation, patience, and encouragement. He has made available his support in a number of ways. I have learned a lot of from him, above all things the manner to face the world. I will never forget his sincerity, dedication and friendship.

It is an honor for me to thank Professor Govind P. Agrawal for his considerable support, expert guidance, supervision and assistant, for the insights he shared me and for patiently answering a great many questions. I owe my deepest gratitude to him for letting me have a good time with his research group at The Institute of Optics, University of Rochester. He made me be part of his research group in all ways. I have learned a lot of from him.

I would like to extend my appreciation to my co-advisor Dr. Daniel Alberto May Arrioja for his advice, recommendation, supervision and assistant throughout the research, and Lic. Silvia Hernández Moreno and Dr. Ponciano Rodríguez Montero for their invaluable support and assistant during my PhD studies at the Instituto Nacional de Astrofísica, Óptica y Electronica.

My sincere appreciation is extended to my committee members: Dr. Jorge Roberto Zurita Sánchez, Dr. Edmundo Antonio Gutiérrez Domínguez, Dr. J. Jesús Escobedo Alatorre, Dr. Rafael Guzmán Cabrera, and Dr. Miguel Ángel Basurto Pensado for their advice and recommendation throughout this dissertation.

I would also like to express my gratitude to all those people who have helped and inspired me throughout my PhD studies. Special thanks to Brian Daniel, Yuzhe Xiao, Jordan Leidner, and Shaival Buch for their assistant, unselfish and unfailing support during my internship at the Institute of Optics, University of Rochester, but mostly for their friendship. I also want to thank Alfonso, Julio Cesar, Karla, Cesar, Gisela and Miguel for their friendship. Many thanks to Omar Santiago and Paloma for their help, friendship and fun. I am also grateful to Mrs. Gina Kern for her friendly support and consideration regarding my internship requirements. She was always very helpful, friendly and very nice. I am very grateful for her considerations. In addition, I would like to express my most sincere gratitude to my former Rector Mrs. Nora Claudia Lusting for her trust in my hometown youth and by creating the opportunity for my educational experience.

I would also like to extend my deepest gratitude to the Consejo Nacional de Ciencia y Tecnología (CONACyT) for its considerable financial

support through the postgraduate scholarship 322196 and register number 235214, and a Beca Mixta for the internship during which most of this PhD thesis work was carried out. In addition, I am also grateful to CONACyT for the research grant CB-2008/101378 that provided the support for the general project where this PhD thesis is included. I am aware that all these supports meant the work and interest of people and to them my warmest gratitude for their interest in our success. They are too many to mention and to be aware of, but in their name let me thank to Mrs. Gabriela Gómez Gutiérrez for my Beca Mixta and those of my classmates, to Q. Regina M. Alarcón Contreras for the funding for the marvelous LAOP Workshop where I managed to meet Prof. Agrawal and to Biol. Martha Patricia Ojeda Carrasco for helping us with our project; to all of you thank you very much.

My very deep gratitude goes to the Consejo de Ciencia y Tecnología del Estado de Puebla (Concytep) for its financial support to present this dissertation through the scholarship named "Becas Tesis Concytep 2015".

Last but not least, I want to thank to my family, who have always been there throughout the lows and the highs with unconditional love and support. I ALSO WANT TO THANK GOD FOR EVERY DAY FOR EVERYTHING THAT HAPPENS FOR ME.

Néstor Lozano Crisóstomo
Santa María Tonantzintla, Puebla, México
December 2015

Abstract

Multi-core fibers (MCFs), through the technique of space-division multiplexing (SDM), are the new type of fibers that promise to overcome the critical transmission capacity barriers and boost the capability of optical fiber communication (OFC) systems. However, when a MCF is considered as a medium for SDM transmission, the linear coupling between the MCF cores is a key feature to be considered and analyzed. The fundamental effects of the linear coupling on the nonlinear mechanisms of light-matter interaction that happen when an optical signal propagates through the MCF cores are still unexamined. This feature is actually the most important problem in MCFs, which promise high technological developments in OFC systems.

In this thesis, we revisit and extend the single-core fiber (SCF) fundamentals and limits (the guided modes characteristics, nonlinear phase shift, nonlinear phase noise, self-phase modulation (SPM), and the size effects of the fiber cores) to a nonlinear directional fiber coupler (NLDFC), as the simplest MCF, described as a collection of two coupled SCFs. We present the results of a theoretical study of the effect of linear coupling on the nonlinear phase shift and frequency spectrum of an initial unchirped optical

pulse propagating through a NLDFC, including the situation when the incoming signal is noisy. We focus on a NLDFC, which is the simplest, but most important, setup of MCFs to obtain physical insight of the effect of linear coupling on the phenomenon of SPM and nonlinear phase noise. For our purposes, the analysis of the elementary switching process in a NLDFC was suffice to obtain considerable and comprehensive results.

We demonstrate spectral narrowing in the propagation of an initial unchirped optical pulse through a NLDFC. Our results show that the linear coupling between both NLDFC cores induces that spectral narrowing. The amount of narrowing of the pulse spectra depend on the peak power of the input optical pulse. We also demonstrate that the linear coupling reduces the nonlinear phase noise of an optical signal when the first maximum transfer of optical power is carried out between both NLDFC cores. This is so because the maximum nonlinear phase shift is reduced when that first coherent interaction between both NLDFC cores results in an exchange of energy for the first time. We describe these results as an overcoming of the linear coupling on SPM effect. In addition, we show that exist a power-dependent critical coupling coefficient that plays a crucial role in the design of a NLDFC.

Contents

Chapter 1

Introduction

The field of optical fiber communication (OFC) is concerned with using light and optical fibers for the transmission of information over long distances at high bandwidths[1 - 2]. Nowadays, long distances refer to thousand kilometers and high bandwidths refers to terabit per second (Tb/s) capacities[3]. However, due to modern communication services, it is necessary to improve the data transport capacity and the reach of OFC systems to solve the continuous increase of data traffic[4]. In other words, it is required to improve the bit rate-distance product, BL, where B is the bit rate and L is the repeater spacing. One way to achieve this is through the improvement of several optical fiber technologies as low-loss optical components, low-noise optical amplifiers, advanced optical fibers, and advanced modulation formats[3]. Another way is

[1] G. P. Agrawal, *Fiber-Optic Communication Systems*, 4th ed. (Wiley, 2010).
[2] L. N. Binh, *Digital Optical Communications* (CRC Press, 2009).
[3] P. J. Winzer and R.-J. Essiambre, "Advanced optical modulation formats," Proc. IEEE, **94**, 952-985 (2006).
[4] R.-J. Essiambre, G. Kramer, P. J. Winzer, G. J. Foschini, and B. Goebel, "Capacity limits of optical fiber networks," J. Lightwave Technol. **28**(4), 662–701 (2010).

through the improvement of our understanding of the behavior of light in optical fiber technologies to optimize the engineering of OFC systems and get the maximum data rates for a given regeneration-free transmission distance (distance where an optical signal is not detected and retransmitted along the propagation path)[3].

The state of the art of OFC systems has advanced dramatically during the last 45 years since the advent of low-loss optical fibers, predicted by K. C. Kao and G. A. Hockham in 1966[5] and later demonstrated by researchers at the Corning Glass Company in 1970[6], and the demonstration of the GaAs semiconductor laser operating continuously at room temperature[7]. Over the period of 1970 to 2015, there have been several generations of OFC systems. Each generation has brought fundamental changes in research that have helped to improve the systems performance further[1].

Current OFC systems can use light pulses to carry information from one place to another[1-3]. Intensity, phase, carrier frequency and polarization are the physical attributes of optical pulses that can be used to carry information. The optical pulses used for this task have high carrier frequencies, in the range of terahertz (THz), in the visible or near-infrared region of the electromagnetic spectrum. Such optical pulses are generated and modulated by optical transmitters at the input end of an OFC link. An optical receiver

---

[1] G. P. Agrawal, *Fiber-Optic Communication Systems*, 4th ed. (Wiley, 2010).

[2] L. N. Binh, *Digital Optical Communications* (CRC Press, 2009).

[3] P. J. Winzer and R.-J. Essiambre, "Advanced optical modulation formats," Proc. IEEE, **94**, 952-985 (2006).

[5] K. C. Kao and G. A. Hockham, "Dielectric-fibre Surface waveguides for optical frequencies," Proc. IEE **113**, 1151-1158 (1966).

[6] F. P. Kapron, D. B. Keck, and R. D. Maurer, "Radiation losses in glass optical waveguides," Appl. Phys. Lett. **17**, 423-425 (1970).

[7] I. Hayashi, M. B. Panish, P. W. Foy, and S. Sumski "Junction lasers which operate continuously at room temperature," Appl. Phys. Lett. **17**, 109-111 (1970).

converts the light pulses received at the output end in electric signals for its corresponding process to obtain the information encoded[2,8].

Three basic types of digital modulation techniques have been widely used in OFC systems: Amplitude Shift Keying (ASK), Frequency Shift Keying (FSK) and Phase Shift Keying (PSK) in which the amplitude, frequency or phase of the optical carrier wave are manipulated to represent information[2]. However, the progress in optical modulation formats has brought additional secondary data modulation formats derived from the basic types of data modulation formats[1-4]. For example, binary PSK (BPSK), quadrature PSK (QPSK) and 8PSK in which the phase of the optical carrier takes two, four, and eight values to represent information. In addition, a hybrid modulation technique named quadrature amplitude modulation (QAM) can be created with the combination of the ASK and PSK optical modulation formats, in which the phase and amplitude of the carrier are changed simultaneously[2]. Nowadays, before schemes of optical modulation and the technique of dense wavelength-division multiplexing (DWDM), which permits the propagation of many carrier waves through an only one optical fiber link[8], have become the key ingredients in the design of high data rate OFC systems.

For long time ASK data modulation format has been used in OFC systems[1]. However, in recent years there has been growing interest in advanced optical modulation formats to build flexible and cost-effective high-

---

[1] G. P. Agrawal, *Fiber-Optic Communication Systems*, 4th ed. (Wiley, 2010).

[2] L. N. Binh, *Digital Optical Communications* (CRC Press, 2009).

[3] P. J. Winzer and R.-J. Essiambre, "Advanced optical modulation formats," Proc. IEEE, **94**, 952-985 (2006).

[4] R.-J. Essiambre, G. Kramer, P. J. Winzer, G. J. Foschini, and B. Goebel, "Capacity limits of optical fiber networks," J. Lightwave Technol. **28**(4), 662–701 (2010).

[8] M. S. Borella, J. P. Jue, D. Banerjee, B. Ramamurthy, and B. Mukherjee, "Optical components for WDM lightwave networks," Proc. IEEE, **85**(8), 1274-1307 (1997).

capacity OFC systems[3]. In particular, schemes that transmit information by modulating the phase of the optical carrier wave have had intense interest[9], where the data modulation formats like binary and quaternary differential PSK (DBPSK/DQPSK) have been the focus of the research community[10 - 11]. This is so because these advanced modulation schemes have greater receiver sensitivity and increased spectral efficiency[8, 12]. Increasing spectral efficiency is often the most economical means to increase DWDM systems capacity[12]. Receiver sensitivity refers to the lowest level, of the parameter that is used to carry information, at which the receiver can detect a signal and demodulate data. Spectral efficiency refers to the data rate that can be transmitted over a given bandwidth. However, the performance of OFC systems that use phase modulation formats varies according to the linear and nonlinear impairments in optical fibers: optical fiber losses, amplified spontaneous emission (ASE) noise, chromatic dispersion, and optical fiber nonlinearities.

Losses in optical fibers are result of the material absorption and scattering[1]. In this sense, the power of optical signals is reduced during their propagation along optical fibers. Therefore, losses in optical fibers limit the reach of OFC systems. To compensate losses in optical fibers, OFC systems use inline optical amplifiers[13]. However, the process of optical amplification introduces ASE noise in the transmitted optical signal field (noise in the

---

1 G. P. Agrawal, *Fiber-Optic Communication Systems*, 4th ed. (Wiley, 2010).

3 P. J. Winzer and R.-J. Essiambre, "Advanced optical modulation formats," Proc. IEEE, **94**, 952-985 (2006).

8 M. S. Borella, J. P. Jue, D. Banerjee, B. Ramamurthy, and B. Mukherjee, "Optical components for WDM lightwave networks," Proc. IEEE, **85**(8), 1274-1307 (1997).

9 A. Demir, "Nonlinear phase noise in optical-fiber-communication systems," J. Lightw. Technol., **25**(8), 2002–2032 (2007).

10 J.-K. Rhee, D. Chowdhury, K. S. Cheng, and U. Gliese, "DPSK 32 ×10 Gb/s transmission modeling on 5 × 90 km terrestrial system," IEEE Photon. Technol. Lett. **12**(12), 1627–1629 (2000).

11 C. Xu, X. Liu, and X. Wei, "Differential phase-shift keying for high spectral efficiency optical transmissions," IEEE J. Sel. Topics Quantum Electron. **10**(2), 281–293 (2004).

12 J. A. Kahn and K.-P. Ho, "Spectral efficiency limits and modulation/detection techniques for DWDM systems," IEEE Journal of Selected Topics in Quantum Electronics **10**(2), 259-272 (2004).

13 E. Desuvire, Erbium-Doped Fiber Amplifiers: Principles and Applications (Wiley, 1994).

amplitude)[9]. The field amplitude fluctuations caused by the noise are translated into phase fluctuations, nonlinear phase noise, because of the optical fiber nonlinearity. Specifically, the optical fiber nonlinearity refers to the phenomenon of self-phase modulation (SPM), which originates from the variation of the refractive index of the guided medium dependent on the launched power. The nonlinear phase noise is detrimental in OFC systems based on BPSK or QPSK, in which the information is encoded in the optical phase, leading to bit errors in transmission systems. In addition, SPM induces spectral broadening of the optical pulses propagating through the optical fiber, leading to distortions in OFC systems that use DWDM.

1.1 Motivation

While single-core fiber (SCF) networks are gradually approaching their theoretical capacity limits[4], new types of fibers such as multi-core fibers (MCFs) have been the focus of worldwide research to overcome critical transmission capacity barriers and boost the capability of the OFC systems[14]. This is so because their signal-carrying capacity is many times greater than that of traditional SCFs and because their multiple core distribution allows working at higher intensities but still within the limits of low intensity SCF. In MCFs, a number of cores is introduced at different positions, in a preselected array, in the fiber cross-section and within a single cladding. In the most typical case, each core accommodates a single guided mode, depending on

---

[4] R.-J. Essiambre, G. Kramer, P. J. Winzer, G. J. Foschini, and B. Goebel, "Capacity limits of optical fiber networks," J. Lightwave Technol. **28**(4), 662–701 (2010).

[9] A. Demir, "Nonlinear phase noise in optical-fiber-communication systems," J. Lightw. Technol., **25**(8), 2002–2032 (2007).

[14] T. Morioka, Y. Awaji, R. Ryf, P. J. Winzer, D. Richardson, and F. Poletti, "Enhancing optical communications with brand new fibers," IEEE Commun. Mag. **50**(2), S31–S42 (2012).

the size of the MCF cores and some other design parameters, but may be a number of guided modes. MCFs have attracted attention for enhancing the capacity of OFC systems through space-division multiplexing (SDM)[15], and several experiments have demonstrated high-speed data transmission over MCFs at rates that approach a petabit per second (Pb/s)[16]. When we consider a MCF as a medium for SDM transmission, the linear coupling between cores is a key feature to be considered[17].

Essential to SCF-OFC systems is the use of optical amplification that however introduces noise in the transmitted optical signal field. The field amplitude fluctuations caused by the noise are translated into phase fluctuations, nonlinear phase noise, because of the SCF nonlinearity. The nonlinear phase noise is detrimental in SCF-OFC systems based on DPSK or QPSK in which the information is encoded in the optical phase, leading to bit errors in transmission systems. Therefore, it is expected that this limitation is extended to MCFs described as a collection of coupled SCFs. One of our purpose in this thesis is to study how the linear coupling affects the nonlinear phase noise in the simplest MCF coupler case, a nonlinear directional fiber coupler (NLDFC), instead of using MCFs that are more complex.

The NLDFC is one of the most exciting components in lightwave technology. Jensen first proposed it in 1982[18]. It consists of two parallel optical fiber cores placed in close proximity. These optical fiber cores, which

---

15 D. J. Richardson, J. M. Fini, and L. E. Nelson, "Space-division multiplexing in optical fibers," Nat. Photonics 7(5), 354–362 (2013).

16 A. Sano, H. Takara, et. al, "409-Tb/s + 409-Tb/s crosstalk suppressed bidirectional MCF transmission over 450 km using propagation-direction interleaving," Opt. Express 21(14), 16777–16783 (2013).

17 K. Nakajima, Y. Goto, T. Matsui, and S. Tomita, "Multi-core fiber technologies for extremely advanced transmission," in Proceedings of IEEE Opto-Electronics and Communications Conference (IEEE, 2011), pp. 248-249.

18 S. M. Jensen, "The nonlinear coherent coupler," IEEE J. Quantum Electron. **QE-18**, 1580-1583 (1982).

form two input and two output ports, utilize the coherent interaction based on evanescent waves to transfer optical power from one optical fiber core to another under suitable condition[19]. The NLDFC consist generally of two regimes: the linear and nonlinear regime. In the linear regime, where the optical power is low or/and there is modal overlap between the adjacent NLDFC cores, neighboring NLDFC cores exchange optical power periodically. In the nonlinear regime, where the optical power is high or/and there is no modal overlap between the adjacent NLDFC cores, the nonlinear effects in each NLDFC core reduce the power exchange between the adjacent NLDFC cores, retaining most optical power in only one NLDFC core.

In particular, the simplest MCF coupler, the NLDFC, plays a quite important role in OFC systems, where it may be conveniently used in the switching of light beams[20 – 21]. An optical pulse propagating in a NLDFC can accumulate significant amount of phase, the nonlinear phase shift, via SPM. The role of the nonlinear phase shift in OFC systems is quite important for information transmission. Added directly to the signal phase, the nonlinear phase shift is intensity-dependent because of the optical fibers Kerr nonlinearity. The key factor associated with the nonlinear phase shift is related with the chirping and spectral changes, spectral broadening of optical pulses that can degrade the performance of NLDFC-based lightwave systems. The SPM-induced spectral change is a consequence of the nonlinear phase shift time dependence, which temporal variation is identical to that of the pulse intensity. Nevertheless, useful devices such as all-optical modulators, switches, splitters, logic gates, and so on can be developed based on the

---

19 G. P. Agrawal, *Applications of Nonlinear Fiber Optics*, 2nd ed. (Academic Press, 2008).

20 C. Pare and M. Florjanczyk, "Approximate model of soliton dynamics in all-optical couplers," Phys. Rev. A **41**, 6287-6295 (1990).

21 Y. Wang and J. Liu, "All-fiber logical devices based on the nonlinear directional coupler," IEEE Phot. Technol. Lett. **11**, 72-74 (1999).

NLDFC, in which such nonlinear phase shift plays a critical role. Therefore, the study of nonlinear phase shift and spectral broadening in NLDFC is quite important.

In general, optical switching consists in enabling signals, which propagate in a NLDFC, to be selectively switch from one fiber core to another under suitable conditions. However, when an optical pulse propagates in a NLDFC, each portion of the optical pulse is selectively switch because the performance of the switching depends on the optical power of the signal, i.e., low-power portions of the optical pulse are switched and high-power portions are retained[22]. This feature of power discrimination has recently attracted considerable attention for mode-locked fiber laser applications[23]. However, in order to fully characterize the performance of optical pulses in NLDFCs and obtain an accurate physical insight of the switching process, the theory of optical switching requires to be improved.

In summary, the single-core fiber fundamentals and limits as the guided modes characteristics, nonlinear phase noise, self-phase modulation, supercontinuum generation, and the size effects of the fiber cores need to be revisited and extended to a NLDFC, as the simplest MCF coupler, described as a collection of two coupled SCFs. In this sense, a NLDFC can be used to study the impact of the linear coupling on the nonlinear mechanisms as SPM and nonlinear phase shift, including the situation when the incoming signal is noisy. Considering the simpler setup of a NLDFC can give more fundamental information and physical insight about the effect of the linear coupling on the

---

22 E. Nazemosadat and A. Mafi, "Saturable absorption in multicore fiber couplers," J. Opt. Soc. Am. B **30** 2787–2790 (2013).

23 H. G. Winful and D. T. Walton, "Passive mode locking through nonlinear coupling in a dual-core fiber laser," Opt. Lett. **17**, 1688–1690 (1992).

nonlinear mechanisms as self-phase modulation and nonlinear phase noise instead of using MCFs that are more complex. In addition, the consequences of the nano-dimensions of the NLDFC cores on the propagation of optical pulses can be analyzed by using the vectorial nature of the guided modes.

1.2 Thesis Contribution

This thesis deals with the analysis of the nonlinear phase noise in NLDFCs and a novel optical nonlinearity compensation technique to partially mitigate SPM in OFC systems. In general, in this thesis the SCF fundamentals and limits as the guided modes characteristics, nonlinear phase noise, SPM, supercontinuum generation, and the size effects of the fiber cores are revisited and extended to a NLDFC, as the simplest MCF coupler, described as a collection of two coupled SCFs. In this sense, a NLDFC is used to study the impact of the linear coupling on the nonlinear mechanisms as SPM and nonlinear phase shift, including the situation when the incoming signal is noisy. We show that the simpler setup of a NLDFC gives more fundamental information and physical insight about the effect of the linear coupling on the nonlinear mechanisms as SPM and nonlinear phase noise instead of using more complex MCFs.

1.3 Thesis outline

In chapter 2, we introduce the important concepts of SCFs that are used to understand and clarify the thesis objective. The purpose of this chapter is to build a conceptual structure that allows to tie together all the key ideas. In

chapter 3, we derive the coupled-mode propagation equations that govern the evolution of the complex envelope of optical pulses along NLDFCs. Here we consider the condition of a single-input excitation for the NLDFCs. In chapter 4, we derive an exact analytical expression for the nonlinear phase shift of an optical pulse propagating in a dispersionless NLDFC. In chapter 5, we analyze the effect of the linear coupling on the nonlinear phase noise in NLDFCs, when a single-input excitation is considered to perform optical switching. In chapter 6, we study the effect of the linear coupling on SPM of an optical pulse propagating through a NLDFC. We analyze the effect of the linear coupling on the shape and spectrum of initially unchirped optical pulses propagating in a dispersionless NLDFC. Finally, we give the conclusions in chapter 7.

References

[1] G. P. Agrawal, Fiber-Optic Communication Systems, 4th ed. (Wiley, 2010).

[2] L. N. Binh, Digital Optical Communications (CRC Press, 2009).

[3] P. J. Winzer and R.-J. Essiambre, "Advanced optical modulation formats," Proc. IEEE, 94, 952-985 (2006).

[4] R.-J. Essiambre, G. Kramer, P. J. Winzer, G. J. Foschini, and B. Goebel, "Capacity limits of optical fiber networks," J. Lightwave Technol. 28(4), 662–701 (2010).

[5] K. C. Kao and G. A. Hockham, "Dielectric-fibre Surface waveguides for optical frequencies," Proc. IEE **113**, 1151-1158 (1966).

[6] F. P. Kapron, D. B. Keck, and R. D. Maurer, "Radiation losses in glass optical waveguides," Appl. Phys. Lett. **17**, 423-425 (1970).

[7] I. Hayashi, M. B. Panish, P. W. Foy, and S. Sumski "Junction lasers which operate continuously at room temperature," Appl. Phys. Lett. **17**, 109-111 (1970).

[8] M. S. Borella, J. P. Jue, D. Banerjee, B. Ramamurthy, and B. Mukherjee, "Optical Components for WDM Lightwave Networks," Proceedings of the IEEE, **85**(8), 1274-1307 (1997).

[9] Demir, "Nonlinear phase noise in optical-fiber-communication systems," J. Lightw. Technol., 25(8), 2002–2032 (2007).

[10] J.-K. Rhee, D. Chowdhury, K. S. Cheng, and U. Gliese, "DPSK 32 ×10 Gb/s transmission modeling on 5 × 90 km terrestrial system," IEEE Photon. Technol. Lett. **12**(12), 1627–1629 (2000).

[11] C. Xu, X. Liu, and X. Wei, "Differential phase-shift keying for high spectral efficiency optical transmissions," IEEE J. Sel. Topics Quantum Electron. **10**(2), 281–293 (2004).

[12] J. A. Kahn and K.-P. Ho, "Spectral efficiency limits and modulation/detection techniques for DWDM systems," IEEE Journal of Selected Topics in Quantum Electronics 10(2), 259-272 (2004).

[13] E. Desuvire, Erbium-Doped Fiber Amplifiers: Principles and Applications (Wiley, 1994).

[14] T. Morioka, Y. Awaji, R. Ryf, P. J. Winzer, D. Richardson, and F. Poletti, "Enhancing optical communications with brand new fibers," IEEE Commun. Mag. **50**(2), S31–S42 (2012).

[15] D. J. Richardson, J. M. Fini, and L. E. Nelson, "Space-division multiplexing in optical fibers," Nat. Photonics **7**(5), 354–362 (2013).

[16] A. Sano, H. Takara, et. al, "409-Tb/s + 409-Tb/s crosstalk suppressed bidirectional MCF transmission over 450 km using propagation-direction interleaving," Opt. Express **21**(14), 16777–16783 (2013).

[17] K. Nakajima, Y. Goto, T. Matsui, and S. Tomita, "Multi-core fiber technologies for extremely advanced transmission," in Proceedings of IEEE Opto-Electronics and Communications Conference (IEEE, 2011), pp. 248-249.

[18] S. M. Jensen, "The nonlinear coherent coupler," IEEE J. Quantum Electron. **QE-18**, 1580-1583 (1982).

[19] G. P. Agrawal, *Applications of Nonlinear Fiber Optics*, 2nd ed. (Academic Press, 2008).

[20] C. Pare and M. Florjanczyk, "Approximate model of soliton dynamics in all-optical couplers," Phys. Rev. A **41**, 6287-6295 (1990).

[21] Y. Wang and J. Liu, "All-fiber logical devices based on the nonlinear directional coupler," IEEE Phot. Technol. Lett. **11**, 72-74 (1999).

[22] E. Nazemosadat and A. Mafi, "Saturable absorption in multicore fiber couplers," J. Opt. Soc. Am. B **30** 2787–2790 (2013).

[23] H. G. Winful and D. T. Walton, "Passive mode locking through nonlinear coupling in a dual-core fiber laser," Opt. Lett. **17**, 1688–1690 (1992).

Chapter 2

Literature Background

Abstract

In this chapter, we introduce the important concepts that are used to understand and clarify the thesis objective. In general, the purpose of this section is to build a conceptual structure that allows to tie together all the key ideas. First in Section 2.1, we give a general overview of the essential of SCFs in OFC systems. In Section 2.2, we describe the characteristics of the SCFs. In addition, the single-mode condition is specified. In Section 2.3, we emphasize the importance of the attenuation losses of SCFs. In Section 2.4, we describe the function of erbium-doped fiber amplifiers (EDFAs) as the components used to compensate the attenuation losses of SCFs. Section 2.5 gives the analysis of the consequence of using EDFAs in OFC systems; the ASE noise. The important concepts of the nonlinear phenomena as optical Kerr effect, SPM, nonlinear phase shift, and the spectral broadening of optical pulses propagating in SCFs are introduced in Section 2.6. Finally, the concept

of nonlinear phase noise as a consequence of the phenomenon of SPM and ASE noise is analyzed in Section 2.7.

2.1 Introduction

Modern OFC systems generally use step-index SCFs, which are characterized by a uniform refractive index within the core and a sharp decrease in the refractive index at the core-cladding interface. In general, a SCF works as a light pipe in which light beams propagate through the core by the phenomenon of total internal reflection, i.e., by a succession of total internal reflections at the boundary between the core and the cladding following a zigzag path. In this sense, a SCF offers, through its cylindrical core of high refractive index, a spatial confinement of light beams over long propagation distances.

2.2 Single-Core Optical Fiber Characteristics

A SCF consist of a cylindrical core of pure silica glass surrounded by a cladding layer whose refractive index n_2 is slightly lower than the refractive index of the core n_1. In general, exist two types of SCFs: 1) single-mode and 2) multimode. The difference between both SCFs is the number of guided modes supported by each one. A single-mode SCF only support one-guide mode, while a multimode SCF support many guided modes. A guide mode in a SCF corresponds geometrically to one path, among the possible paths, in which an optical beam can propagate through the optical fiber (see Fig. 2.1b). More formally, a guide mode corresponds to a solution of the wave

equation that is derived from Maxwell's equations and subject to boundary conditions imposed by the SCF[1 - 2].

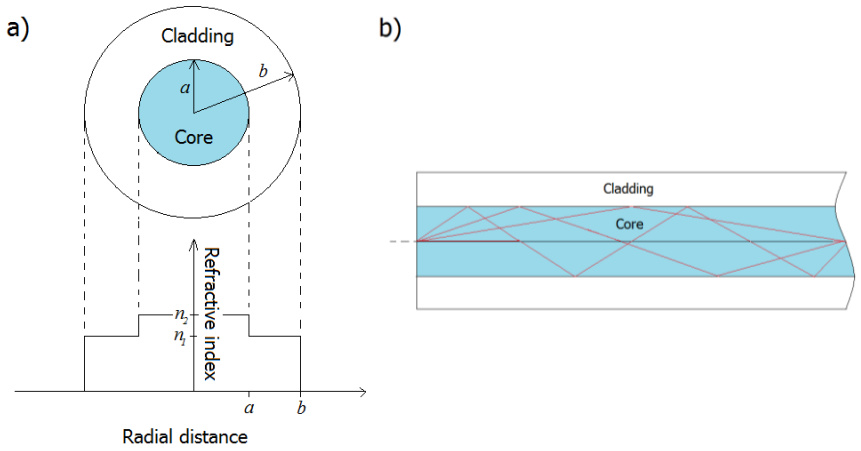

Fig. 2.1 a) Cross section and refractive index profile for step-index SCFs. b) Light confinement through total internal reflection in step-index SCFs.

An optical pulse propagating along a SCF is defined by an electric field vector **E** and a magnetic field vector **H**. Each field can be broken down into three components. These components are E_x, E_y, E_z, H_x, H_y, and H_z, where z is the component of the field that is in the direction of propagation. Guided modes typically are referred to using the notation HE_{xy} (if $H_z > E_z$), or EH_{xy} (if $E_z > H_z$), where x and y are both integers. For the case x=0, the guided modes are referred to as transverse-electric (TE), in which case $E_z = 0$, or transverse-magnetic (TM), in which case $H_z = 0$[3 - 4].

---

[1] G. P. Agrawal, *Fiber-Optic Communication Systems*, 4th ed. (Wiley, 2010).
[2] A. Yariv and P. Yeh, *Photonics: Optical Electronics in Modern Communications*, 6th ed. (Oxford University Press, 2006).
[3] G. P. Agrawal, *Nonlinear Fiber Optics*, 5th ed. (Academic Press, 2013).
[4] M. S. Borella, J. P. Jue, D. Banerjee, B. Ramamurthy, and B. Mukherjee, "Optical Components for WDM Lightwave Networks," Proceedings of the IEEE, **85**(8), 1274-1307 (1997).

Two important parameters physically characterize a SCF. The relative core-cladding index difference $\Delta = (n_1 - n_2)/n_1$ and the so-called V parameter defined as $V = a\, k_0 (n_1^2 - n_1^2)^{1/2}$, where $k_0 = 2\pi/\lambda$, a is the core radius, and λ is the carrier wavelength of light[3]. The value of V defines the number of guided modes supported by a SCF (see Fig. 2.2). In this sense, the number of guided modes supported by a SCF at a given wavelength depends on its design parameters, namely the core radius and refractive index of the core and cladding. Therefore, a larger core radius or high operating frequency allows a greater number of guided modes to propagate through a SCF.

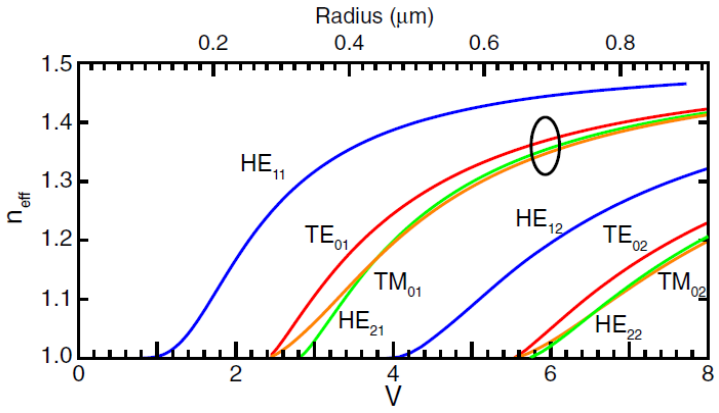

Fig. 2.2 Effective index of refraction for the lowest lying guide modes in a SCF versus the parameter V (bottom axis) and core radius (top axis)[5].

2.2.1 Single-mode condition of single-core fibers

A SCF support only the HE_{11} guided mode, also referred as the fundamental mode, when $V<2.405$[3]. This condition is obtained in part by reducing the

[3] G. P. Agrawal, *Nonlinear Fiber Optics*, 5th ed. (Academic Press, 2013).

[5] J. E. Hoffman, F. K. Fatemi, G. Beadie, S. L. Rolston, and L. A. Orozco, "Rayleigh scattering in an optical nanofiber as a probe of higher-order mode propagation," Optica **2**, 416-423 (2015).

core to a sufficiently small diameter such that the SCF only captures one guide mode. One result of this condition is a high confinement of light into very small spatial dimensions.

In general, the transverse distribution F(x,y) of the fundamental guide mode HE_{11} over the x-y plane, can be approximated by a Gaussian distribution of the form [3]

$$F(x,y) = \exp[-(x^2 + y^2)/w^2], \tag{2.1}$$

where w is the mode width parameter related with the parameter V by [3]

$$w/a \approx 0.65 + 1.619V^{-3/2} + 2.879V^{-6}. \tag{2.2}$$

2.3 Single-Core Fiber Losses

The development and innovation for both the SCF and laser are very important for the increase in the capacity of OFC systems. Nowadays, most of the commercially available SCFs have losses below 0.2 dB/km in the 1.55 μm wavelength region[6]. In this sense, light pulses can be transmitted through SCFs for a long distance without optical amplification. However, when the length of an OFC link exceeds a certain value, in the range of 20–100 km depending on the operating wavelength, it becomes necessary to compensate the SCF losses at the end of the optical SCF link because the signal pulses become too weak to be detected reliably[1].

---

[1] G. P. Agrawal, *Fiber-Optic Communication Systems*, 4th ed. (Wiley, 2010).
[3] G. P. Agrawal, *Nonlinear Fiber Optics*, 5th ed. (Academic Press, 2013).
[6] K.-P. Ho, *Phase-Modulated Optical Communication Systems*, (Springer, 2005).

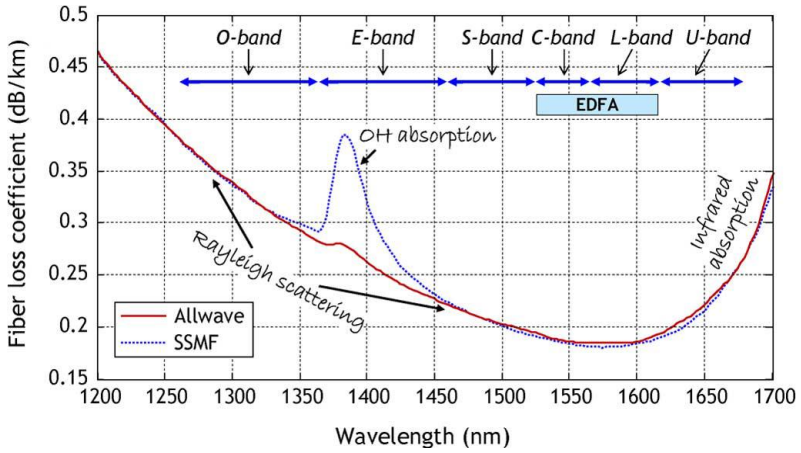

Fig. 2.3 Measured attenuation in silica fibers (purple line) and theoretical limits (red line) given by Rayleigh scattering in the short-wavelength region, and by molecular vibrations (infrared absorption) in the infrared spectral region[7].

The attenuation loss parameter for optical fibers α in units of dB/km is given by the following relation

$$\alpha_{dB/km} = -\frac{10}{L}\log\left(\frac{P_{out}}{P_{in}}\right), \tag{2.3}$$

where L is the length of the optical fiber, P_{in} is the launched optical power, and P_{out} is the output power given by

$$P_{out} = P_{in}\exp(-\alpha L), \tag{2.4}$$

where $\alpha = 0.23\alpha_{dB/km}$ is the attenuation constant.

[7] R.-J. Essiambre, G. Kramer, P. J. Winzer, G. J. Foschini, and B. Goebel, "Capacity limits of optical fiber networks," J. Lightwave Technol. **28**(4), 662–701 (2010).

2.4 Compensation of Fiber Losses

Fiber attenuation losses are compensated by using optical amplifiers, which amplify the optical signal directly without requiring conversion of the signal to the electric domain as it was done before 1990[8].

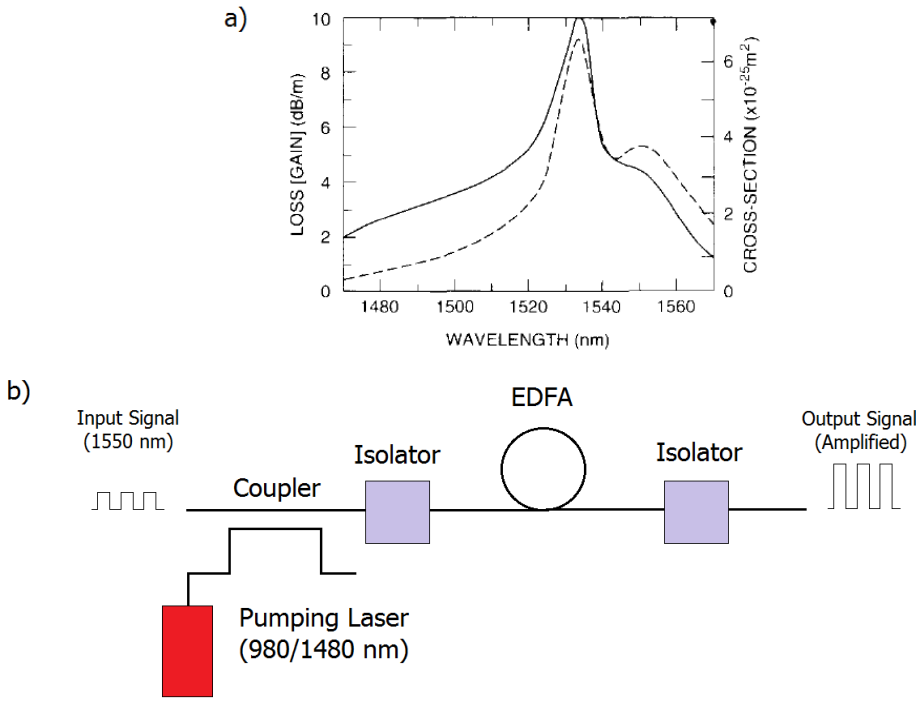

Fig. 2.4 a) Absorption and gain spectra of an EDFA whose core was doped with erbium ions (Er^{3+}) and GeO_2 [9]. b) Typical configuration of EDFA based OFC system.

Most OFC systems actually employ inline EDFAs in which attenuation losses accumulated over 60 to 80 km of fiber lengths are compensated using

[8] L. Kazovsky, S. Benedetto, and A. Willner, *Optical Fiber Communications Systems* (Artech House, Inc, 1996).
[9] C. R. Giles and E. Desurvire, "Modeling Erbium-Doped Fiber Amplifiers," J. Lightwave Techno. **9**, 271-283 (1991).

short lengths around 10 m of erbium-doped fibers[10]. This is so because erbium-doped fibers provide gain at the low-loss spectral window around 1.55 μm[11]. The EDFAs are pumped at 0.98 μm or 1.48 μm in OFC systems. They have a typical gain in the range of 20-40 dB from a few meters of fiber, but the gain varies significantly with wavelength[2] (see Fig. 2.4a).

2.5 Amplified Spontaneous Emission Noise

The EDFAs have been applied broadly nowadays in OFC systems due to their significant features. One important feature is to enable the use of the technique of DWDM, which led to the development of systems with capacities exceeding 10 Tb/s. However, there is a problem when they are used; the addition of ASE noise to the amplified signal pulses[1].

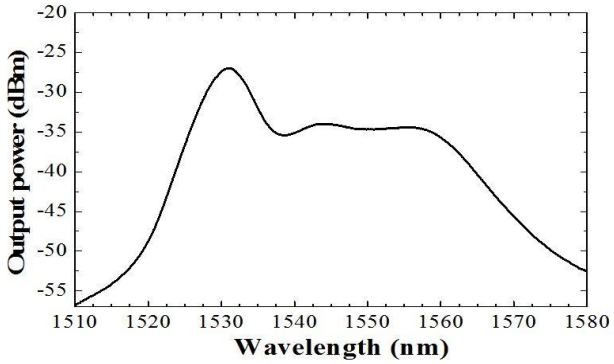

Fig. 2.5 ASE noise obtained from a 1 m length of Er-80 when it is pumped by a 980 nm light source[12].

---

[1] G. P. Agrawal, *Fiber-Optic Communication Systems*, 4th ed. (Wiley, 2010).

[2] A. Yariv and P. Yeh, Photonics: Optical Electronics in Modern Communications, 6th ed. (Oxford University Press, 2006).

[10] P. C. Becker, N. A. Olsson, and J. R. Simpson, *Erbium-Doped Fiber Amplifiers: Fundamentals and Technology* (Academic Press, 1999).

[11] E. Desuvire, *Erbium-Doped Fiber Amplifiers: Principles and Applications* (Wiley, 1994).

[12] http://www.intechopen.com/books/current-developments-in-optical-fiber-technology/multi-wavelength-fiber-lasers

The physical origin of this noise is the spontaneous emission that occurs just after the positive population inversion in the pumped erbium-doped fibers. The transition due to spontaneous emission produces photons with similar energies than the signal photons, but without the same physical properties. These photons do not contribute to the amplification of the signal pulses but rather contribute adding noise to the signal through its amplification by stimulated emission.

2.6 Optical Fiber Nonlinearities

The availability of low-loss optical fibers and optical amplifiers led not only to a revolution in the field of OFC but also to advent of the new field of nonlinear fiber optics[3]. The term nonlinear in the field of optical fibers refers to the nonlinear response of optical fibers to an intense electromagnetic field. When optical signals propagate through an optical fiber, they suffer a distortion due to nonlinearity. The shape, spectrum and phase are the features of optical pulses that are distorted. The Kerr effect is the dominant nonlinear phenomenon in optical fibers. It refers to the change in the refractive index of silica glass due to intense electromagnetic fields[13]. The intensity dependence of the refractive index is given as

$$n(t) = n_0 + n_2 I(t), \tag{2.5}$$

[3] G. P. Agrawal, *Nonlinear Fiber Optics*, 5th ed. (Academic Press, 2013).
[13] R. H. Stolen and A. Ashkin, "Optical Kerr effect in glass waveguide", Appl. Phys. Lett. **22**, 294 (1973)

where n_0 is the linear part of the refractive index, n_2 is the nonlinear-index coefficient, $I(t) = P(t)/A_{eff}$ is the optical intensity, $P(t)$ is the optical power inside the optical fiber, and A_{eff} is the effective area of the optical fiber core.

The nonlinear part of the refractive index $n_2 I(t)$ governs most of the nonlinear effects in optical fibers[3]. When an optical pulse propagates through an optical fiber, the higher intensity portions of an optical pulse encounter a higher refractive index of the optical fiber because the Kerr effect. Silica glass does not exhibit a high nonlinearity because n_2 is small compared to most other nonlinear media. The nonlinear-index coefficient n_2 is $3x10^{-20}\,m^2/W$. However, optical fibers offer strong spatial confinement of light in very small dimensions such that its intensity is enhanced (see Eq. (2.5)). As a result, the nonlinearity is also enhanced because the nonlinear Kerr effect. Because the relatively long lengths over which optical fibers can maintain high optical intensities, nonlinear effects are important. Nonlinear effects in DWDM-OFC systems are routinely observed even at mW power levels.

2.6.1 Self-phase modulation

In particular, phenomenon of SPM refers to a manifestation of the intensity dependence of the refractive index in nonlinear optical media like optical fibers, i.e., it is a consequence of the optical Kerr effect[14]. Specifically, SPM is the change in the phase of an optical pulse resulting from the nonlinearity of

[3] G. P. Agrawal, *Nonlinear Fiber Optics*, 5th ed. (Academic Press, 2013).
[14] R. H. Stolen and C. Lin, "Self-phase-modulation in silica optical fibers," Phys. Rev. A **17**, 1448 (1978).

the refractive index of the optical fiber. Therefore, the phase shift is intensity depended. Here an explication of the SPM phenomenon.

2.6.1.1 Nonlinear phase shift

Consider the simplest situation in which a single optical pulse of the form $A(0,T)$ is launched into a dispersionless single-mode SCF. Here, $T = t - z/v_g$, is the time measured in the frame of reference moving with the pulse at the group velocity v_g. The origin of the nonlinear phenomenon comes from the definition of the propagation constant $\beta = nk_0$, which using Eq. (2.5) can be written as

$$\beta(T) = \beta_0 + \frac{k_0 n_2}{A_{eff}} P(T), \tag{2.6}$$

where $\beta_0 = n_0 k_0$ is the linear propagation constant. Here the optical power is defined as $P(T) = |A(0,T)|^2$. The total phase shift of an optical pulse due to SPM after a distance L of propagation is given by

$$\phi_{NL}(L,T) = \int_0^L \beta - \beta_0 dz, \tag{2.7}$$

where the z-axis is the direction of propagation. Substituting Eq. (2.6) into (2.7) and assuming no optical fiber losses, we obtain

$$\phi_{NL}(L,T) = \gamma P(T) L, \tag{2.8}$$

where $\gamma = k_0 n_2 / A_{eff}$ is nonlinear coefficient. Equation (2.8) gives the amount of phase that an optical pulse can accumulate via SPM. The nonlinear phase shift changes with time in exactly the same way as the optical pulse. Therefore, the optical pulse at the output can be written as

$$A(L,T) = A(0,T)\exp[i\phi_{NL}(L,T)]. \tag{2.9}$$

As we can see in Eq. (2.9), SPM induce a nonlinear phase shift in an optical pulse. The nonlinear phase shift depends on the power of the launch optical pulse and increase with the propagation distance of the pulse. The nonlinear phase shift increases with the nonlinear constant as well. The maximum nonlinear phase shift occurs at the pulse center located at T=0, and is given by

$$\phi_{NLmax}(L) = \gamma P_0 L, \tag{2.10}$$

where $P_0 = P(0)$ is the peak power of the input optical pulse.

2.6.1.2 Spectral broadening of optical pulses

SPM induce spectral broadening in optical pulses when they propagate through SCFs[3,15]. This is so because of the time dependence of the nonlinear phase shift (see Eq. (2.8)), i.e., the variation of the instantaneous frequency across the pulse from its central frequency value ω_0. To

[3] G. P. Agrawal, *Nonlinear Fiber Optics*, 5th ed. (Academic Press, 2013).
[15] G. S. He and S. H. Liu, Physics of Nonlinear Optics (World Scientific, 1999).

demonstrate this phenomenon, we consider again the propagation of a single pulse of light inside a dispersionless single-mode SCF. At the entrance of the optical fiber, we launch a unchirped Gaussian pulse of the form:

$$A(0,T) = A_0 \exp\left(-\frac{T^2}{2T_0^2}\right), \tag{2.11}$$

where T_0 is the pulse width, and A_0 is the constant amplitude such that $|A_0|^2 = P_0$.

The spectral content of the optical pulse at the output of the optical fiber of length L, is obtained by taking the Fourier transform of Eq. (2.9) and using Eq. (2.11). This is given by

$$S(\omega,L) = \left|\int_{-\infty}^{\infty} A(0,T)\exp[i\phi_{NL}(L,T) + i(\omega-\omega_0)T]dT\right|^2. \tag{2.12}$$

Figure 2.6 shows the spectra of an unchirped Gaussian pulse for several values of L, i.e., for different values of the maximum phase shift ϕ_{NLmax}. Here the following values for the calculation are used: $P_0 = 0.1$ W, and $\gamma = 2$ km^{-1}W^{-1}. It is clear to notice that SPM creates new frequencies and leads to spectral broadening. Spectral broadening is accompanied with an oscillatory structure covering the entire frequency range. The number of peak depends on L (ϕ_{NLmax}) and increase linearly with it. SPM-induced spectral broadening can degrade the performance of OFC systems that use the technique of DWDM.

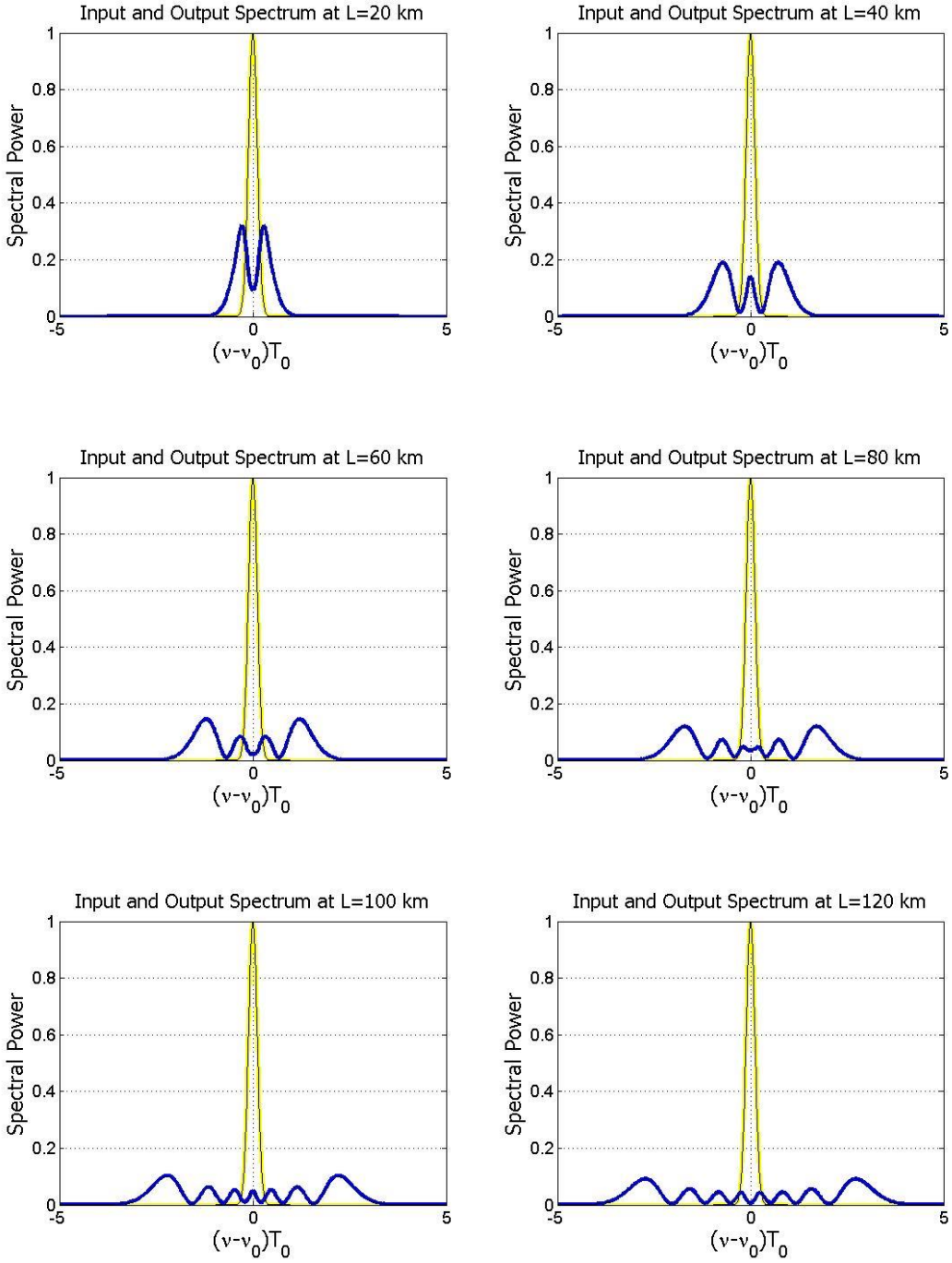

Fig. 2.6 Output spectra (blue curve) of an unchirped Gaussian pulse for different lengths of the dispersionless single-mode SCF. The input spectra are specified by the yellow curve.

2.7 Nonlinear Phase Noise

Consider an optical signal propagating through an OFC system with N inline EDFAs. The electric field at the output of the OFC system can be represented by

$$\mathbf{E} = \mathbf{E}_0 + \mathbf{n}_1 + \ldots + \mathbf{n}_N, \tag{2.13}$$

where $\mathbf{n}_j$ with j=1,…,N represents the jth noise component of the electric field. Therefore, the output nonlinear phase noise is given by

$$\phi_{NL} = \gamma L\left[\left|\mathbf{E}_0 + n_1\right|^2 + \left|\mathbf{E}_0 + n_1 + n_2\right|^2 + \ldots + \left|\mathbf{E}_0 + n_1 + \ldots + n_N\right|^2\right]. \tag{2.14}$$

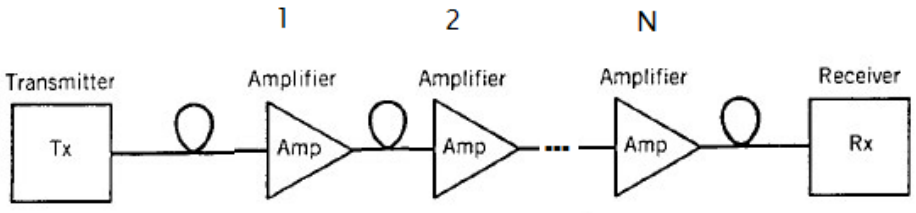

Fig. 2.7 OFC system with N inline EDFAs.

In summary, when EDFAs are used to compensate for optical fiber losses in OFC systems, the field amplitude fluctuations caused by the ASE noise are translated into phase fluctuations, nonlinear phase noise, because of the optical fiber nonlinearity[16]. The nonlinear phase noise degrades OFC systems that use phase modulation as the principal format to transmit information, limiting the regeneration-free transmission distance.

---

[16] J. P. Gordon and L. F. Mollenauer, "Phase noise in photonic communications systems using linear amplifiers," Opt. Lett. **15**, 1351-1353 (1990).

References

[1] G. P. Agrawal, *Fiber-Optic Communication Systems*, 4th ed. (Wiley, 2010).

[2] A. Yariv and P. Yeh, Photonics: Optical Electronics in Modern Communications, 6th ed. (Oxford University Press, 2006).

[3] G. P. Agrawal, *Nonlinear Fiber Optics*, 5th ed. (Academic Press, 2013).

[4] M. S. Borella, J. P. Jue, D. Banerjee, B. Ramamurthy, and B. Mukherjee, "Optical Components for WDM Lightwave Networks," Proceedings of the IEEE, **85**(8), 1274-1307 (1997).

[5] J. E. Hoffman, F. K. Fatemi, G. Beadie, S. L. Rolston, and L. A. Orozco, "Rayleigh scattering in an optical nanofiber as a probe of higher-order mode propagation," Optica 2, 416-423 (2015).

[6] K.-P. Ho, *Phase-Modulated Optical Communication Systems*, (Springer, 2005).

[7] R.-J. Essiambre, G. Kramer, P. J. Winzer, G. J. Foschini, and B. Goebel, "Capacity limits of optical fiber networks," J. Lightwave Technol. 28(4), 662–701 (2010).

[8] L. Kazovsky, S. Benedetto, and A. Willner, Optical Fiber Communications Systems (Artech House, Inc, 1996).

[9] C. R. Giles and E. Desurvire, "Modeling Erbium-Doped Fiber Amplifiers," J. Lightwave Techno. **9**, 271-283 (1991).

[10] P. C. Becker, N. A. Olsson, and J. R. Simpson, Erbium-Doped Fiber Amplifiers: Fundamentals and Technology (Academic Press, 1999).

[11] E. Desuvire, *Erbium-Doped Fiber Amplifiers: Principles and Applications* (Wiley, 1994).

[12] http://www.intechopen.com/books/current-developments-in-optical-fiber-technology/multi-wavelength-fiber-lasers

[13] R. H. Stolen and A. Ashkin, "Optical Kerr effect in glass waveguide", Appl. Phys. Lett. **22**, 294 (1973).

[14] R. H. Stolen and C. Lin, "Self-phase-modulation in silica optical fibers," Phys. Rev. A **17**, 1448 (1978).

[15] G. S. He and S. H. Liu, *Physics of Nonlinear Optics* (World Scientific, 1999).

[16] J. P. Gordon and L. F. Mollenauer, "Phase noise in photonic communications systems using linear amplifiers," Opt. Lett. **15**, 1351-1353 (1990)

Chapter 3

Pulse Propagation in Nonlinear Directional Fiber Couplers

Abstract

In this chapter, we derive the coupled-mode propagation equations that govern the evolution of the complex envelope of optical pulses along NLDFCs. In this regard, a NLDFC made of two identical single-mode highly nonlinear fiber cores is considered such that the vectorial nature of the propagating modes must be applicable. Section 3.1 introduces the theoretical elements to consider for the nonlinear processes in NLDFCs. In Section 3.2, the Maxwell's equations and important concepts such as the Poynting's theorem, which it is used to express the electromagnetic power flow along NLDFCs, and the linear and nonlinear induced polarization are introduced. In addition, an operator Schrödinger-like equation that completely describes the spatial evolution of

an electromagnetic field through an optical medium like a NLDFC is introduced too. In Section 3.3, the concepts of propagating modes of fiber cores, normalization and the coupled-mode approach to solve the operator Schrödinger-like equation are discussed. The coupled-mode equations for a NLDFC are given in Section 3.4.

3.1 Introduction

For an understanding of the coupling and nonlinear phenomena in NLDFCs, it is necessary to consider the theory of electromagnetic wave propagation in dispersive nonlinear media[1]. In the investigation of the nonlinear processes in NLDFCs, we must deal with sufficiently intense light launched into any NLDFC core such that the optical properties of the NLDFC depend on the intensity and other characteristics of the light waves. Alternatively, to examine the behavior of the nonlinear wave propagation along NLDFCs, we need to consider the linear and nonlinear coupling between the propagating modes of both NLDFC cores and the induced polarization, and we can do this last by introducing the induced polarization as a source term in Maxwell's equations.

3.2 Electromagnetic Vectorial Theory

Consider the rational theory for the propagation of light that was developed by Maxwell in the 1860s. The equations for the electric field vector **E** and magnetic field vector **H** in MKS units are given by

[1] G. P. Agrawal, *Applications of Nonlinear Fiber Optics*, 2nd ed. (Academic Press, 2008).

$$\nabla \times \mathbf{E} = -\mu_0 \partial_t \mathbf{H} - \partial_t \mathbf{M}, \tag{3.1}$$

$$\nabla \times \mathbf{H} = \varepsilon_0 \partial_t \mathbf{E} + \partial_t \mathbf{P}, \tag{3.2}$$

where μ_0 is the vacuum permeability, ε_0 is the vacuum permittivity, and **P** and **M** are the induced electric and magnetic polarizations. For optical fibers **M**=0. Maxwell's equations can be used to obtain a plausible relationship between an electromagnetic wave and its energy content[2-3]. To derive this relationship, we subtract the scalar product of the electric field **E** and Eq. (3.2) from the scalar product of the magnetic field **H** and Eq. (3.1), and integrate both sides over a volume V. The following equation is obtained:

$$\int_V [\mathbf{H} \cdot (\nabla \times \mathbf{E}) - \mathbf{E} \cdot (\nabla \times \mathbf{H})] dV = -\int_V [\mu_0 (\mathbf{H} \cdot \partial_t \mathbf{H}) + \varepsilon_0 (\mathbf{E} \cdot \partial_t \mathbf{E}) + (\mathbf{E} \cdot \partial_t \mathbf{P})] dV. \tag{3.3}$$

Using the vector identity $\nabla \cdot (\mathbf{E} \times \mathbf{H}) = \mathbf{H} \cdot (\nabla \times \mathbf{E}) - \mathbf{E} \cdot (\nabla \times \mathbf{H})$ and noting that $\mathbf{H} \cdot \partial_t \mathbf{H} = \frac{1}{2} \partial_t (\mathbf{H} \cdot \mathbf{H})$ and $\mathbf{E} \cdot \partial_t \mathbf{E} = \frac{1}{2} \partial_t (\mathbf{E} \cdot \mathbf{E})$, Eq. (3.3) becomes

$$-\int_S \mathbf{E} \times \mathbf{H} \cdot \hat{\mathbf{n}} dS = \int_V \left(\frac{\mu_0}{2} \partial_t |\mathbf{H}|^2 + \frac{\varepsilon_0}{2} \partial_t |\mathbf{E}|^2 + \mathbf{E} \cdot \partial_t \mathbf{P} \right) dV, \tag{3.4}$$

where $\hat{\mathbf{n}}$ is the outward-directed unit vector normal to the surface S enclosing V. Here we have used the divergence theorem for the vector $\mathbf{E} \times \mathbf{H}$. In Eq. (3.4), the first term on the right-hand side represents the rate of

---

2 M. Born and E. Wolf, *Principles of Optics*, 7th ed. (Cambridge University Press, 1999).

3 A. Yariv and P. Yeh, *Photonics: Optical Electronics in Modern Communications*, 6th ed. (Oxford University Press, 2007).

increase of the magnetic stored energy, the second term represents the rate of increase of the electric stored energy, and the last term represents the power per unit volume expended by the electric field on the electric dipoles that are formed in the optical medium[3 – 4]. Therefore, the left-hand side of Eq. (3.4) represents the total electromagnetic power flow into the volume V bounded by S. If we replace $\hat{\mathbf{n}}$ by the inward-directed unit vector in the z direction $\hat{\mathbf{z}} = -\hat{\mathbf{n}}$, the total power of the electromagnetic wave flowing in the z direction, out of the volume V bounded by S, can be expressed by

$$P = \int_S \mathbf{S} \cdot \hat{\mathbf{z}} dS, \tag{3.5}$$

where $\mathbf{S} = \mathbf{E} \times \mathbf{H}$[W/m²] is the Poynting vector that represents the electromagnetic power flow density[3 – 5].

The general second-order wave equation for the propagation of an electromagnetic wave through an optical dielectric medium, valid for both linear and nonlinear characterization, can be obtained by taking the curl of Eq. (3.1) and using Eq. (3.2), that is

$$\nabla \times \nabla \times \mathbf{E} = -\frac{1}{c^2} \partial_t^2 \mathbf{E} - \mu_0 \partial_t^2 \mathbf{P}, \tag{3.6}$$

where c is the speed of light in vacuum and we have used the relation $\mu_0 \varepsilon_0 = 1/c^2$.

---

[3] A. Yariv and P. Yeh, *Photonics: Optical Electronics in Modern Communications*, 6th ed. (Oxford University Press, 2007).
[4] K. Okamoto, *Fundamentals of Optical Waveguides*, 2nd ed. (Academic Press, 2006).
[5] A. W. Snyder and J. D. Love, *Optical Waveguide Theory* (Kluwer Academic, 2000).

The nature of the optical medium is exhibited by the relation between **P** and **E**, called the medium equation. On a fundamental level, the origin of the nonlinear response of an optical medium is related to the anharmonic motion of the bound electrons under the influence of an applied optical field[6 – 7]. Because **M**=0 for optical fibers[8], there are not nonlinear terms in the magnetic field **H**. As a result, the total electric dipole-moment density **P** is not linear in the electric field **E**, but satisfies the more general relation[6 – 8]

$$\mathbf{P} = \varepsilon_0 \chi^{(1)} \cdot \mathbf{E} + \varepsilon_0 \chi^{(2)} : \mathbf{EE} + \varepsilon_0 \chi^{(3)} \vdots \mathbf{EEE} + \ldots, \tag{3.7}$$

where $\chi^{(j)}$ (j=1,2,3,…) is the jth order susceptibility. In general, $\chi^{(j)}$ is a tensor of rank j+1. Here it is convenient to split **P** into its linear and nonlinear parts as $\mathbf{P} = \mathbf{P}^{L} + \mathbf{P}^{NL}$, where $\mathbf{P}^{L}$ is the part of the induced polarization that depends linearly on the electric field **E**, and $\mathbf{P}^{NL}$ has a nonlinear field dependence.

Introducing **E**, in terms of its Fourier transform through the relation

$$\mathbf{E}(\mathbf{r}, t) = \frac{1}{2\Pi} \int_{-\infty}^{+\infty} \tilde{\mathbf{E}}(\mathbf{r}, \omega) \exp(-i\omega t) d\omega, \tag{3.8}$$

as well as a similar relation for **P** in Eq. (3.6), we obtain a vector wave equation in the Fourier space that is valid for each frequency component of the field:

---

6 Y. R. Shen, *Principles of Nonlinear Optics* (John Wiley & Sons, 1984).
7 P. N. Butcher and D. N. Cotter, *The Elements of Nonlinear Optics* (Cambridge University Press, 1990).
8 R. W. Boyd, *Nonlinear Optics,* 3rd ed. (Academic Press, 2008).

$$\nabla\times\nabla\times\tilde{\mathbf{E}}-n^2k_0^2\tilde{\mathbf{E}}=\omega^2\mu_0\tilde{\mathbf{P}}^{NL}, \tag{3.9}$$

where $k_0=\omega/c$ is the free-space wavenumber and ω is the angular frequency of the electromagnetic wave. Here we have used the relation $\tilde{\mathbf{P}}^{L}=\varepsilon_0\chi^{(1)}\cdot\tilde{\mathbf{E}}$, which is the definition of the Fourier transform of the induced polarization of first order. In general, for silica glass $\chi^{(1)}(\mathbf{r},\omega)$ is assumed a scalar and related with the linear part of the refractive index profile $n(\mathbf{r},\omega)$ of the whole system through $n^2(\mathbf{r},\omega)=1+\chi^{(1)}(\mathbf{r},\omega)$[9]. For $\tilde{\mathbf{P}}^{NL}$ in Eq. (2.9), since $\chi^{(2)}(\mathbf{r},\omega)=0$ for an isotropic medium such a glass[7 – 9], we can only consider the third-order induced polarization and approximate the total electric dipole-moment density by $\tilde{\mathbf{P}}^{NL}\approx\tilde{\mathbf{P}}^{(3)}$, where $\tilde{\mathbf{P}}^{(3)}=\varepsilon_0\chi^{(3)}\vdots\tilde{\mathbf{E}}\tilde{\mathbf{E}}\tilde{\mathbf{E}}$.

When we consider an optical pulse with a carrier frequency ω_0, propagating through an optical dielectric medium in which the linear refractive index is dependent on frequency, $\mathbf{E}$ and $\mathbf{P}^{(3)}$ can be expressed as

$$\mathbf{E}(\mathbf{r},t)=\frac{1}{2}[\boldsymbol{E}(\mathbf{r},t)e^{-i\omega_0 t}+c.c.], \tag{3.10}$$

$$\mathbf{P}^{(3)}(\mathbf{r},t)=\frac{1}{2}[\boldsymbol{P}^{(3)}(\mathbf{r},t)e^{-i\omega_0 t}+c.c.], \tag{3.11}$$

where c.c denotes the complex conjugate. Note that we have separated the rapidly varying part of $\mathbf{E}$ and $\mathbf{P}^{(3)}$. Therefore,

---

[7] P. N. Butcher and D. N. Cotter, *The Elements of Nonlinear Optics* (Cambridge University Press, 1990).
[8] R. W. Boyd, *Nonlinear Optics,* 3rd ed. (Academic Press, 2008).
[9] G. P. Agrawal, *Nonlinear Fiber Optics,* 5th ed. (Academic Press, 2013).

$$\tilde{\mathbf{E}}(\mathbf{r},\omega)=\frac{1}{2}[\tilde{\boldsymbol{E}}(\mathbf{r},\omega-\omega_0)+\text{c.c.}], \tag{3.12}$$

$$\tilde{\mathbf{P}}^{(3)}(\mathbf{r},\omega)=\frac{1}{2}[\tilde{\boldsymbol{P}}^{(3)}(\mathbf{r},\omega-\omega_0)+\text{c.c.}]. \tag{3.13}$$

Substituting Eqs. (3.12) and (3.13) in Eq. (3.9), we obtain the nonlinear wave equation for the Fourier transform of the electric slowly varying amplitude $\tilde{\boldsymbol{E}}$:

$$\nabla\times\nabla\times\tilde{\boldsymbol{E}}-n^2k_0^2\tilde{\boldsymbol{E}}=\omega^2\mu_0\tilde{\boldsymbol{P}}^{(3)}, \tag{3.14}$$

where $\tilde{\boldsymbol{P}}^{(3)}$ is only a small perturbation of the linear wave equation. Analogously, if the magnetic field is defined as $\mathbf{H}(\mathbf{r},t)=\frac{1}{2}[\boldsymbol{H}(\mathbf{r},t)e^{-i\omega_0 t}+\text{c.c.}]$, the nonlinear wave equation for the Fourier transform of the magnetic slowly varying amplitude $\tilde{\boldsymbol{H}}$ can be written as

$$\nabla\times\frac{1}{\varepsilon}\nabla\times\tilde{\boldsymbol{H}}-k_0^2\tilde{\boldsymbol{H}}=-i\omega\nabla\times\frac{1}{\varepsilon}\tilde{\boldsymbol{P}}^{(3)}, \tag{3.15}$$

where $\varepsilon(\mathbf{r},\omega)=n^2(\mathbf{r},\omega)$ is the dielectric constant of the medium. Because optical fiber cores are longitudinally homogeneous and transversely inhomogeneous media, $\varepsilon(\mathbf{r},\omega)=\varepsilon(x,y,\omega)$ and the flow of the electromagnetic energy is only along the guiding structure and not perpendicular to it. Equations (3.14) and (3.15) are the general slowly varying amplitude equations that governs the propagation of an electromagnetic field in a NLDFC.

It results be useful to rewrite Eqs. (3.14) and (3.15) as an operator Schrödinger-like equation that completely describes the spatial evolution of an electromagnetic field through an optical medium like a NLDFC. This linear operator formalism allows to directly establish the normalization property of guided modes of the NLDFC cores[10 - 11]. To obtain the operator equation, we first make a distinction between the transverse and longitudinal components of the Fourier transform of the electric slowly varying amplitude, magnetic slowly varying amplitude and third-order dipole-moment density as $\tilde{\boldsymbol{E}} = \tilde{\boldsymbol{E}}_{\mathrm{T}} + \hat{\mathbf{z}}\tilde{E}_{\mathrm{z}}$, $\tilde{\boldsymbol{H}} = \tilde{\boldsymbol{H}}_{\mathrm{T}} + \hat{\mathbf{z}}\tilde{H}_{\mathrm{z}}$, and $\tilde{\boldsymbol{P}}^{(3)} = \tilde{\boldsymbol{P}}_{\mathrm{T}}^{(3)} + \hat{\mathbf{z}}\tilde{P}_{\mathrm{z}}^{(3)}$. Making a similar distinction for the nabla and Laplacian operators as $\nabla = \nabla_{\mathrm{T}} + \hat{\mathbf{z}}\partial_{\mathrm{z}}$ and $\nabla^2 = \nabla_{\mathrm{T}}^2 + \partial_{zz}$, respectively, Eqs. (3.14) and (3.15) can be rewritten as (see Appendix A for its derivation)

$$-\mathrm{i}\partial_{\mathrm{z}}\hat{\mathrm{F}}\left|\Psi_{\mathrm{T}}\right\rangle = \hat{\mathrm{H}}\left|\Psi_{\mathrm{T}}\right\rangle + \left|\mathrm{P}\right\rangle, \tag{3.16}$$

where $\left|\Psi_{\mathrm{T}}\right\rangle$ is a vector space that contains the transverse fields $\tilde{\boldsymbol{H}}_{\mathrm{T}}$ and $\tilde{\boldsymbol{E}}_{\mathrm{T}}$, and is given by

$$\left|\Psi_{\mathrm{T}}\right\rangle = \begin{pmatrix} \sqrt{\varepsilon_0}\,\tilde{\boldsymbol{E}}_{\mathrm{T}} \\ \sqrt{\mu_0}\,\tilde{\boldsymbol{H}}_{\mathrm{T}} \end{pmatrix}. \tag{3.17}$$

The $\hat{\mathrm{F}}$ and $\hat{\mathrm{H}}$ operators are given by

---

10 A. D. Bresler, G. H. Joshi, and N. Marcuvitz, "Orthogonality properties for modes in passive and active uniform wave guides," J. Appl. Phys **29**, 794-799 (1958).

11 B. A. Daniel, D. N. Maywar, and G. P. Agrawal, "Dynamic mode theory of optical resonators undergoing refractive index changes," J. Opt. Soc. Am. B **28**, 2207-2215 (2011).

$$\hat{F} = \begin{pmatrix} 0 & -\hat{\mathbf{z}}\times \\ \hat{\mathbf{z}}\times & 0 \end{pmatrix}, \tag{3.18}$$

$$\hat{H} = \begin{pmatrix} \frac{\omega}{c}n^2 - \frac{c}{\omega}\nabla_T \times \nabla_T \times & 0 \\ 0 & \frac{\omega}{c} - \frac{c}{\omega}\nabla_T \times \frac{1}{n^2}\nabla_T \times \end{pmatrix}. \tag{3.19}$$

In the theory of nonlinear fiber optics, the nonlinear term $\tilde{\boldsymbol{P}}^{(3)}$ usually is treated as a small perturbation to the linear terms in the electromagnetic field. Here the perturbative term $|P\rangle$ is given by

$$|P\rangle = \begin{pmatrix} \omega\sqrt{\mu_0}\tilde{\boldsymbol{P}}_T^{(3)} \\ -i\frac{1}{\sqrt{\varepsilon_0}}\nabla_T \times \hat{\mathbf{z}}\frac{1}{\varepsilon}\tilde{P}_z^{(3)} \end{pmatrix}. \tag{3.20}$$

The overlap between, or inner product of, two vector spaces $|\Psi_{Tn}\rangle$ and $|\Psi_{Tm}\rangle$, is the number $\langle\Psi_{Tn}|\Psi_{Tm}\rangle$ given by

$$\langle\Psi_{Tn}|\Psi_{Tm}\rangle = \int\int_{-\infty}^{+\infty}(\varepsilon_0\tilde{\boldsymbol{E}}_{Tn}^{*}\cdot\tilde{\boldsymbol{E}}_{Tm} + \mu_0\tilde{\boldsymbol{H}}_{Tn}^{*}\cdot\tilde{\boldsymbol{H}}_{Tm})dxdy = \delta_{nm}, \tag{3.21}$$

which express the normalization and orthogonality condition for the vector spaces $|\Psi_{Tn}\rangle$ and $|\Psi_{Tm}\rangle$. Here δ_{nm} is the Kronecker delta that is defined as: $\delta_{nm} = 1$ if m=n and $\delta_{nm} = 0$ if $m \neq n$. If $\delta_{nm} = 0$, the vector spaces $|\Psi_{Tn}\rangle$ and $|\Psi_{Tm}\rangle$ are orthogonal. If $\delta_{nm} = 1$, then the vector space $|\Psi_{Tn}\rangle$ is said to be normalized.

3.3 Formulation of Guided Modes of Two Parallel Fiber Cores

3.3.1 Fiber core modes

Optical fiber cores can support a finite number of guided modes[9,12] which spatial distribution is a solution of Eq. (3.16) with $|P\rangle = 0$ and satisfies all appropriate boundary conditions. Optical modes supported by any fiber core in the absence of other fiber core can be represented by

$$|\Psi_n\rangle = |\beta_n\rangle e^{i\beta_n z}, \tag{3.22}$$

where $\beta_n(\omega)$ is the propagation constant or eigenvalue of the nth mode, and $|\beta_n\rangle$ the eigenmode defined as:

$$|\beta_n\rangle = \begin{pmatrix} \sqrt{\varepsilon_0}\mathbf{e}_n \\ \sqrt{\mu_0}\mathbf{h}_n \end{pmatrix}. \tag{3.23}$$

Here $\mathbf{e}_n = \mathbf{e}_{Tn} + \hat{\mathbf{z}}e_{zn}$ and $\mathbf{h}_n = \mathbf{h}_{Tn} + \hat{\mathbf{z}}h_{zn}$ are the electric and magnetic modal profiles of the nth mode of the fiber core, respectively. For simplicity, we approximate the electric and magnetic modal profiles with their value at the carrier frequency ω_0, i.e., we assume that the modal profiles do not change significantly over the pulse bandwidth.

---

[9] G. P. Agrawal, *Nonlinear Fiber Optics,* 5th ed. (Academic Press, 2013).
[12] A. Ghatak and K. Thyagarajan, *Introduction to fiber optics* (Cambridge University Press, 1997).

In this work, we only consider fiber cores supporting the fundamental mode. To find the transverse modal profile of the fundamental mode of each fiber core, we need to solve the following equation:

$$-i\partial_z \hat{F}\left|\Psi_{Tm}\right\rangle = \hat{H}_m\left|\Psi_{Tm}\right\rangle, \tag{3.24}$$

where the operator $\hat{H}_m$ is given by

$$\hat{H}_m = \begin{pmatrix} \frac{\omega}{c}n_m^2 - \frac{c}{\omega}\nabla_T \times \nabla_T \times & 0 \\ 0 & \frac{\omega}{c} - \frac{c}{\omega}\nabla_T \times \frac{1}{n_m^2}\nabla_T \times \end{pmatrix}, \tag{3.25}$$

and m=1,2. Here m represents the number of fiber cores that form the NLDFC and n_m is the linear refractive index of the mth fiber core.

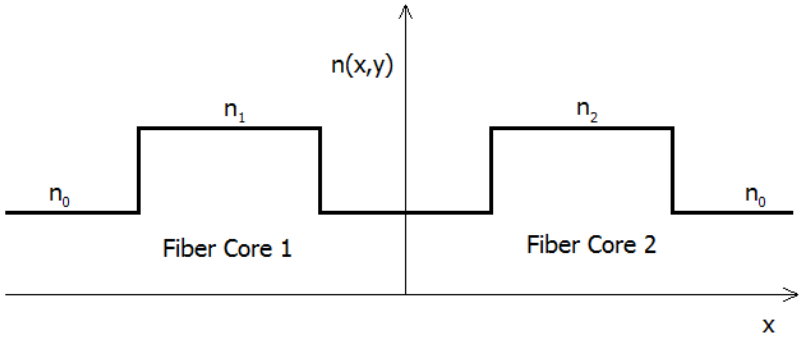

Fig 3.1 Refractive index distribution n of the NLDFC. n_1 and n_2 are the linear refractive indexes of each NLDFC core, and n_0 is the linear refractive index of the cladding.

The longitudinal part of the fundamental mode of the mth fiber core

$$\left|\Psi_{zm}\right\rangle = \begin{pmatrix} \sqrt{\varepsilon_0}\tilde{E}_{zm} \\ \sqrt{\mu_0}\tilde{H}_{zm} \end{pmatrix}, \tag{3.26}$$

can be obtained using $\left|\Psi_{Tm}\right\rangle$ and the Maxwell's equations. Decomposing the eigenmode $\left|\beta_m\right\rangle$ into transverse and longitudinal components, the vector space that contains the mode fields $\tilde{\boldsymbol{H}}_m$ and $\tilde{\boldsymbol{E}}_m$ is given by

$$\left|\Psi_m\right\rangle = \left|\Psi_{Tm}\right\rangle + \hat{\mathbf{z}}\left|\Psi_{zm}\right\rangle = \left|\beta_{Tm}\right\rangle e^{i\beta_m z} + \hat{\mathbf{z}}\left|\beta_{zm}\right\rangle e^{i\beta_m z}, \tag{3.27}$$

where

$$\left|\beta_{Tm}\right\rangle = \begin{pmatrix} \sqrt{\varepsilon_0}\mathbf{e}_{Tm} \\ \sqrt{\mu_0}\mathbf{h}_{Tm} \end{pmatrix}, \tag{3.28}$$

$$\left|\beta_{zm}\right\rangle = \begin{pmatrix} \sqrt{\varepsilon_0}e_{zm} \\ \sqrt{\mu_0}h_{zm} \end{pmatrix}. \tag{3.29}$$

Substituting the corresponding transversal part of Eq. (3.27) into Eq. (3.24), we obtain the following eigenvalue equation for the transversal part of the eigenmode $\left|\beta_m\right\rangle$:

$$\hat{H}_m\left|\beta_{Tm}\right\rangle = \beta_m\hat{F}\left|\beta_{Tm}\right\rangle. \tag{3.30}$$

Because we are considering normal modes of the fiber cores with a $\exp(i\beta_m z)$ z-dependence, we can replace the $\hat{F}$ operator in Eq. (3.24) by the following operator relation when $\tilde{\boldsymbol{P}}^{(3)} = 0$ (see Appendix B for its derivation):

$$-i\partial_z \hat{F}\left|\Psi_{Tm}\right\rangle = \partial_z \hat{N}_m \left|\Psi_{zm}\right\rangle - \partial_z^2 \hat{Z}_m \left|\Psi_{Tm}\right\rangle. \tag{3.31}$$

In this regard, we can take into consideration the effects caused by the nonlinear terms in β_m in Eq. (3.24). The $\hat{N}_m$ and $\hat{Z}_m$ operators are given by

$$\hat{N}_m = \begin{pmatrix} \frac{c}{\omega}\nabla_T & 0 \\ 0 & \frac{c}{\omega}\frac{1}{n_m^2}\nabla_T \end{pmatrix}, \tag{3.32}$$

$$\hat{Z}_m = \begin{pmatrix} \frac{c}{\omega} & 0 \\ 0 & \frac{c}{\omega}\frac{1}{n_m^2} \end{pmatrix}. \tag{3.33}$$

Substituting the corresponding transversal and longitudinal part of Eq. (3.27) into Eq. (3.31), we obtain the following relation:

$$\hat{F}\left|\beta_{Tm}\right\rangle = i\hat{N}_m \left|\beta_{zm}\right\rangle + \beta_m \hat{Z}_m \left|\beta_{Tm}\right\rangle. \tag{3.34}$$

Equation (3.34) shows the relation between the longitudinal and transverse components of the electromagnetic field mode. Multiplying Eq. (3.34) by $\left\langle\beta_{Tk}\right|$ with k=1,2 from the left, we obtain

$$\left\langle \beta_{Tk} \middle| \hat{F} \middle| \beta_{Tm} \right\rangle = \frac{1}{c}\int\int_{-\infty}^{+\infty} (\mathbf{e}_{Tm} \times \mathbf{h}_{Tk}^{*} + \mathbf{e}_{Tk}^{*} \times \mathbf{h}_{Tm}) \cdot \hat{\mathbf{z}} dxdy = \begin{cases} \dfrac{4N_m}{c} & \text{if } k = m \\ \dfrac{C_{km}}{c} & \text{if } k \neq m \end{cases}, \quad (3.35)$$

where C_{km} is an arbitrary parameter. This is so because, in general, fundamental modes supported by the two NLDFC cores are not orthogonal. If the field modes $\left|\beta_{Tm}\right\rangle$ and $\left|\beta_{Tk}\right\rangle$ were orthogonal, then $C_{km} = 0$.

Applying the definitions of the electric and magnetic field in the slowly varying envelope approximation (Eqs. (3.10) and (3.11)) to Eq. (3.5), we can note that the parameter N_m represents the time average of the mth mode power flow in the propagation direction. The parameter N_m is defined as

$$N_m = \frac{1}{2}\int\int_{-\infty}^{+\infty} \mathrm{Re}\{(\mathbf{e}_m \times \mathbf{h}_m^{*}) \cdot \hat{\mathbf{z}}\} dxdy, \quad (3.36)$$

where $(\mathbf{e}_{Tm} \times \mathbf{h}_{Tm}^{*}) \cdot \hat{\mathbf{z}} = (\mathbf{e}_m \times \mathbf{h}_m^{*}) \cdot \hat{\mathbf{z}}$. Moreover, we obtain the following relations for the electric and magnetic field modes:

$$\begin{aligned} &\int\int_{-\infty}^{+\infty} (\mathbf{e}_{Tk}^{*} \times \mathbf{h}_{Tm}) \cdot \hat{\mathbf{z}} dxdy \\ &\quad = \frac{1}{k_0}\sqrt{\frac{\varepsilon_0}{\mu_0}}\int\int_{-\infty}^{+\infty} (\beta_m \mathbf{e}_{Tk}^{*} \cdot \mathbf{e}_{Tm} + i\mathbf{e}_{Tk}^{*} \cdot \nabla_T e_{zm}) dxdy, \end{aligned} \quad (3.37)$$

$$\begin{aligned}&\iint_{-\infty}^{+\infty}(\mathbf{e}_{Tm}\times\mathbf{h}_{Tk}^{*})\cdot\hat{\mathbf{z}}\,dxdy\\&\quad=\frac{1}{k_0}\sqrt{\frac{\mu_0}{\varepsilon_0}}\iint_{-\infty}^{+\infty}\left(\frac{1}{n_m^2}\beta_m\mathbf{h}_{Tk}^{*}\cdot\mathbf{h}_{Tm}+i\frac{1}{n_m^2}\mathbf{h}_{Tk}^{*}\cdot\nabla_T h_{zm}\right)dxdy.\end{aligned}\tag{3.38}$$

From Maxwell's equations, one can deduce that electric and magnetic of the mth field modes $\mathbf{e}_m$ and $\mathbf{h}_m$ and the vector in the direction of wave propagation $\hat{\mathbf{z}}$ are mutually orthogonal, and $\mathbf{e}_m$ and $\mathbf{h}_m$ are related by

$$n_m\mathbf{e}_{Tm}=\sqrt{\frac{\mu_0}{\varepsilon_0}}\mathbf{h}_m.\tag{3.39}$$

Therefore,

$$\begin{aligned}&\iint_{-\infty}^{+\infty}(\mathbf{e}_{Tm}\times\mathbf{h}_{Tk}^{*})\cdot\hat{\mathbf{z}}\,dxdy\\&\quad=\frac{1}{k_0}\sqrt{\frac{\varepsilon_0}{\mu_0}}\iint_{-\infty}^{+\infty}\left(\frac{n_k}{n_m}\beta_m\mathbf{e}_{Tk}^{*}\cdot\mathbf{e}_{Tm}+i\frac{n_k}{n_m}\mathbf{e}_{Tk}^{*}\cdot\nabla_T e_{zm}\right)dxdy.\end{aligned}\tag{3.40}$$

3.3.2 Coupled mode theory

Couple-mode theory deals with the simplest formulation that describes the mutual lightwave interactions between two propagation modes. It is used commonly for directional couplers because it addresses systems where the

total field can be described approximately with a linear combination of two propagating modes[1,3–5,13]. To derive the coupled-mode equations that describe the propagation of electromagnetic waves through NLDFCs, we use the coupled-mode approach to solve the operator Schrödinger-like equation given by Eq. (3.16).

The total optical field in the NLDFC is expressed by a linear combination of the two guided modes that corresponds to the modes of the uncopled fiber cores, with an infinite separation between them, which form the NLDFC. Every guided mode is a solution of the Maxwell's equations of each NLDFC core and do not satisfy the Maxwell's equations of the whole system. Considering only the fundamental mode of each NLDFC core as forward-propagating mode, which travel in the positive z-direction, solution of Eq. (3.16) can be expressed by

$$\left|\Psi_{T}\right\rangle = \tilde{a}_1\left|\Psi_{T1}\right\rangle + \tilde{a}_2\left|\Psi_{T2}\right\rangle, \tag{3.41}$$

where $\tilde{a}_m(z,\omega)$ is the modal amplitude in the frequency domain of the mth NLDFC core. The coupling between modes (1) and (2) is expressed by the z-dependence of $\tilde{a}_1$ and $\tilde{a}_2$. The complete vector space solution is given by $\left|\Psi\right\rangle = \left|\Psi_{T}\right\rangle + \hat{\mathbf{z}}\left|\Psi_{z}\right\rangle$. Here we are considering the addition of the modes of two parallel fiber cores together each other with propagation constants evaluated

---

[1] G. P. Agrawal, *Applications of Nonlinear Fiber Optics*, 2nd ed. (Academic Press, 2008).

[3] A. Yariv and P. Yeh, *Photonics: Optical Electronics in Modern Communications*, 6th ed. (Oxford University Press, 2007).

[4] K. Okamoto, *Fundamentals of Optical Waveguides*, 2nd ed. (Academic Press, 2006).

[5] A. W. Snyder and J. D. Love, *Optical Waveguide Theory* (Kluwer Academic, 2000).

[13] C. Vassallo, *Optical Waveguide Concepts* (Elsevier, 1991).

at the carrier frequency ω_0, i.e., we are considering unperturbed field modes, which represents the electromagnetic fields of narrowband pulses at frequency ω_0 for which dispersion, loss, and nonlinearity terms are zero, to represent the total perturbed field of the NLDFC.

Vectorial modal fields $\mathbf{e}_m$ and $\mathbf{h}_m$ on the perturbed and unperturbed fiber cores can be treated as similar functions. Therefore, the field of the NLDFC can be well approximated by

$$\left|\Psi_T\right\rangle = \tilde{a}_1\left|\beta_{T1}\right\rangle e^{i\beta_1 z} + \tilde{a}_2\left|\beta_{T2}\right\rangle e^{i\beta_2 z}, \tag{3.42}$$

where $\beta_m(\omega)$ is the mth perturbed propagation constant of the mode in the mth NLDFC core. Introduction of the mth slowly varying mode amplitude is given by the relation

$$\tilde{a}_m(z,\omega) = \tilde{A}_m(z,\omega-\omega_0)e^{-i(\beta_m-\beta_{0m})z}, \tag{3.43}$$

where $\beta_{0m} = \beta_m(\omega_0)$ is the mth unperturbed propagation constant of the mode in the mth NLDFC core.

3.4 Coupled-Mode Equations for Nonlinear Directional Fiber Couplers

In order to calculate the longitudinal evolution of the complex amplitudes $\tilde{a}_1$ and $\tilde{a}_2$ along the NLDFC, we derive the coupled-mode equations based on

the perturbation theory applied to NLDFCs. For simplicity, we use Eq. (3.16) only applicable for the electric field. In this regard, Eq. (3.16) can be particularly rewritten as

$$\nabla_T \times (\nabla_T \times \tilde{\boldsymbol{E}}_T) + \partial_z \nabla_T \tilde{E}_z - \partial_z^2 \tilde{\boldsymbol{E}}_T - n^2 k_0^2 \tilde{\boldsymbol{E}}_T = \omega^2 \mu_0 \tilde{\boldsymbol{P}}_T^{(3)}, \tag{3.44}$$

where we have use the relation: $i\omega\mu_0 \partial_z(\hat{\mathbf{z}} \times \tilde{\boldsymbol{H}}_T) = \partial_z \nabla_T \tilde{E}_z - \partial_{zz} \tilde{\boldsymbol{E}}_T$ (see Maxwell relations in Appendix A). The relation $\nabla_T \times [\partial_z(\hat{\mathbf{z}} \times \tilde{\boldsymbol{E}}_T)] + \nabla_T \times [\nabla_T \times (\hat{\mathbf{z}} \tilde{E}_z)] = \hat{\mathbf{z}} n^2 k_0^2 \tilde{E}_z + \hat{\mathbf{z}} \omega^2 \mu_0 \tilde{P}_z^{(3)}$ can be used to obtain the most general relation for $\tilde{\boldsymbol{E}}$

$$\begin{aligned} &\nabla_T \times (\nabla_T \times \tilde{\boldsymbol{E}}_T) + \nabla_T \times [\partial_z(\hat{\mathbf{z}} \times \tilde{\boldsymbol{E}}_T)] + \nabla_T \times [\nabla_T \times (\hat{\mathbf{z}} \tilde{E}_z)] \\ &= n^2 k_0^2 \tilde{\boldsymbol{E}} - \partial_z \nabla_T \tilde{E}_z + \partial_z^2 \tilde{\boldsymbol{E}}_T + \omega^2 \mu_0 \tilde{\boldsymbol{P}}^{(3)}. \end{aligned} \tag{3.45}$$

If we consider that a single input pulse, at the carrier frequency ω_0, is launched into one NLDFC core such that it excites a single mode of the NLDFC core, the Fourier transform of the electric field $\tilde{\boldsymbol{E}}$ can be expressed in a similar way like Eq. (3.42), i.e.,

$$\tilde{\boldsymbol{E}}(\mathbf{r}, \omega - \omega_0) = \sum_{m=1}^{2} \tilde{a}_m(z, \omega) \mathbf{F}_m(x, y, \omega_0) e^{i\beta_m z}, \tag{3.46}$$

where $\mathbf{F}_m(x, y, \omega_0) = \mathbf{e}_m(x, y, \omega_0) / \sqrt{N_m}$ governs the shape of the mth mode in the absence of other modes. Substituting Eq. (3.46) into (3.45) and applying the slowly varying envelope approximation, we obtain after associating term:

$$
\begin{aligned}
-\mu_0\omega^2 e^{-i\beta_m z}\tilde{\boldsymbol{P}}^{(3)} = &\sum_{m=1}^{2}(2i\beta_m\mathbf{F}_{Tm} - \nabla_T F_{zm} - \hat{\mathbf{z}}\nabla_T\cdot\mathbf{F}_{Tm})\partial_z\tilde{a}_m \\
&+ i\sum_{m=1}^{2}\beta_m(i\beta_m\mathbf{F}_{Tm} - \nabla_T F_{zm} - \hat{\mathbf{z}}\nabla_T\cdot\mathbf{F}_{Tm})\tilde{a}_m \\
&+ \sum_{m=1}^{2}[\nabla_T^2\mathbf{F}_m - \nabla_T(\nabla_T\cdot\mathbf{F}_{Tm}) + k_0^2 n^2\mathbf{F}_m]\tilde{a}_m,
\end{aligned}
\tag{3.47}
$$

where $\nabla = \nabla_T + \hat{\mathbf{z}}\partial_z$, $\nabla_T = \hat{\mathbf{x}}\partial_x + \hat{\mathbf{y}}\partial_y$, $\mathbf{F}_m = \mathbf{F}_{Tm} + \hat{\mathbf{z}}F_{zm}$, and $\mathbf{F}_{Tm} = \hat{\mathbf{x}}F_{xm} + \hat{\mathbf{y}}F_{ym}$. Here F_{zm} is the longitudinal component and $\mathbf{F}_{Tm}$ is the transverse part of the mth normalized mode field. In the above equation, we have applied the vector identity $\nabla_T\times(\nabla_T\times\tilde{\boldsymbol{E}}_T) = \nabla_T(\nabla_T\cdot\tilde{\boldsymbol{E}}_T) - \nabla_T^2\tilde{\boldsymbol{E}}_T$.

The distribution of the mth electric field mode can be obtained by using Eq. (3.31) only applicable for the electric field mode. Its distribution satisfies:

$$
\nabla_T^2\mathbf{F}_m - \nabla_T(\nabla_T\cdot\mathbf{F}_{Tm}) = -i\beta_m(i\beta_m\mathbf{F}_{Tm} - \nabla_T F_{zm} - \hat{\mathbf{z}}\nabla_T\cdot\mathbf{F}_{Tm}) - k_0^2 n_m^2\mathbf{F}_m. \tag{3.48}
$$

Substituting Eq. (3.48) into the last term on the right-hand side of Eq. (3.47) and associating terms, we obtain

$$
\begin{aligned}
-\mu_0\omega^2 e^{-i\beta_m z}\tilde{\boldsymbol{P}}^{(3)} = &\sum_{m=1}^{2}(2i\beta_m\mathbf{F}_{Tm} - \nabla_T F_{zm} - \hat{\mathbf{z}}\nabla_T\cdot\mathbf{F}_{Tm})\partial_z\tilde{a}_m \\
&+ k_0^2\sum_{m=1}^{2}(n^2 - n_m^2)\mathbf{F}_m\tilde{a}_m.
\end{aligned}
\tag{3.49}
$$

If we multiply Eq. (3.49) by $\mathbf{F}_k^*$ from the left, use the vectorial identity $F_{zk}^*(\nabla_T \cdot \mathbf{F}_{Tm}) = \nabla_T \cdot (F_{zk}^* \mathbf{F}_{Tm}) - \mathbf{F}_{Tm} \cdot \nabla_T F_{zk}^*$, and integrate over the transverse plane, Eq. (3.49) becomes

$$\sum_{m=1}^{2} \partial_z \tilde{a}_m \int\int_{-\infty}^{+\infty} (2i\beta_m \mathbf{F}_{Tk}^* \cdot \mathbf{F}_{Tm} - \mathbf{F}_{Tk}^* \cdot \nabla_T F_{zm} + \mathbf{F}_{Tm} \cdot \nabla_T F_{zk}^*) dxdy$$

$$+ k_0^2 \sum_{m=1}^{2} \tilde{a}_m \int\int_{-\infty}^{+\infty} \Delta n_m^2 \mathbf{F}_k^* \cdot \mathbf{F}_m dxdy \qquad (3.50)$$

$$= -\mu_0 \omega^2 e^{-i\beta_m z} \int\int_{-\infty}^{+\infty} \mathbf{F}_k^* \cdot \tilde{\boldsymbol{P}}^{(3)} dxdy,$$

where $\Delta n_m^2 = n^2 - n_m^2$ is the change in the linear refractive index due to the presence of the mth guide mode. Here we are considering that the integral $\int\int_{-\infty}^{+\infty} \nabla_T \cdot (F_{zk}^* \mathbf{F}_{Tm}) dxdy = 0$ because all guided modes decay exponentially in the cladding. Simplification of Eq. (3.45) is something complicated because both guided modes in the NLDFC are not orthogonal in general. However, if we add Eq. (3.37) and its complex conjugate, i.e.,

$$\frac{i\omega\mu_0}{\sqrt{N_m N_k}} \int\int_{-\infty}^{+\infty} (\mathbf{e}_k^* \times \mathbf{h}_m) \cdot \hat{\mathbf{z}} dxdy = \int\int_{-\infty}^{+\infty} (i\beta_m \mathbf{F}_{Tk}^* \cdot \mathbf{F}_{Tm} - \mathbf{F}_{Tk}^* \cdot \nabla_T F_{zm}) dxdy, \quad (3.51)$$

$$\frac{i\omega\mu_0}{\sqrt{N_m N_k}} \int\int_{-\infty}^{+\infty} (\mathbf{e}_m \times \mathbf{h}_k^*) \cdot \hat{\mathbf{z}} dxdy = \int\int_{-\infty}^{+\infty} (i\beta_k \mathbf{F}_{Tk}^* \cdot \mathbf{F}_{Tm} + \mathbf{F}_{Tm} \cdot \nabla_T F_{zk}^*) dxdy, \quad (3.52)$$

we obtain

$$\int\int_{-\infty}^{+\infty} 2i\beta_m \mathbf{F}_{Tk}^* \cdot \mathbf{F}_{Tm} dxdy - \int\int_{-\infty}^{+\infty} \mathbf{F}_{Tk}^* \cdot \nabla_T F_{zm} dxdy + \int\int_{-\infty}^{+\infty} \mathbf{F}_{Tm} \cdot \nabla_T F_{zk}^* dxdy. \\ = \frac{i\omega\mu_0}{\sqrt{N_m N_k}} \int\int_{-\infty}^{+\infty} (\mathbf{e}_m \times \mathbf{h}_k^* + \mathbf{e}_k^* \times \mathbf{h}_m) \cdot \hat{\mathbf{z}} dxdy, \tag{3.53}$$

where we have considered that the modes are perfectly matched, i.e., $\beta_k = \beta_m$. Substituting Eq. (3.53) into (3.50), we obtain

$$\sum_{m=1}^{2} \partial_z \tilde{a}_m \frac{1}{\sqrt{N_m N_k}} \int\int_{-\infty}^{+\infty} (\mathbf{e}_m \times \mathbf{h}_k^* + \mathbf{e}_k^* \times \mathbf{h}_m) \cdot \hat{\mathbf{z}} dxdy \\ -i\omega\varepsilon_0 \sum_{m=1}^{2} \tilde{a}_m \int\int_{-\infty}^{+\infty} \Delta n_m^2 \mathbf{F}_k^* \cdot \mathbf{F}_m dxdy \\ = i\omega e^{-i\beta_m z} \int\int_{-\infty}^{+\infty} \mathbf{F}_k^* \cdot \tilde{\boldsymbol{P}}^{(3)} dxdy. \tag{2.54}$$

If we introduce the slowly varying mode amplitude $\tilde{A}_m(z, \omega - \omega_0)$ given in Eq. (3.43) into Eq. (3.54), we obtain

$$\sum_{m=1}^{2} \left[\partial_z \tilde{A}_m - i(\beta_m - \beta_{0m}) \tilde{A}_m \right] \frac{1}{\sqrt{N_m N_k}} \int\int_{-\infty}^{+\infty} (\mathbf{e}_m \times \mathbf{h}_k^* + \mathbf{e}_k^* \times \mathbf{h}_m) \cdot \hat{\mathbf{z}} dxdy \\ -i\omega\varepsilon_0 \sum_{m=1}^{2} \tilde{A}_m \int\int_{-\infty}^{+\infty} \Delta n_m^2 \mathbf{F}_k^* \cdot \mathbf{F}_m dxdy \\ = i\omega e^{-i\beta_{0m} z} \int\int_{-\infty}^{+\infty} \mathbf{F}_k^* \cdot \tilde{\boldsymbol{P}}^{(3)} dxdy. \tag{3.55}$$

The last three terms shown in Eq. (3.55) correspond respectively to the dispersion, linear coupling and nonlinearity.

Equation (3.55) describes the evolution of each spectral component ω within the pulse spectrum along then NLDFC. However, we are interested in the evolution of the whole pulse envelope $A_m(z,t)$. Therefore, we rewrite Eq. (3.55) into the time domain. For this purpose, we replace the propagation constant β_m with its Taylor expansion around ω_0 as:

$$\beta_m(\omega) = \sum_{n=0}^{\infty} \frac{\beta_{nm}}{n!}(\omega - \omega_0)^n, \tag{3.56}$$

where β_{nm} are the dispersion coefficients defined as $\beta_{nm} = \partial_\omega^n \beta_m\big|_{\omega=\omega_0}$. In addition, if we replace $\omega - \omega_0$ with $i\partial_t$ and multiplying both sides of Eq. (3.55) by $e^{-i\omega t}$ and integrate with respect to ω, we obtain

$$\begin{aligned}
&\sum_{m=1}^{2}\left(\partial_z A_m - \sum_{n=1}^{\infty} i^{n+1}\frac{\beta_{nm}}{n!}\partial_t^n A_m\right)\frac{1}{\sqrt{N_m N_k}}\int\int_{-\infty}^{+\infty}(\mathbf{e}_m \times \mathbf{h}_k^* + \mathbf{e}_k^* \times \mathbf{h}_m)\cdot\hat{\mathbf{z}}\,dxdy \\
&-i\omega_0\varepsilon_0\sum_{m=1}^{2} A_m\int\int_{-\infty}^{+\infty}\Delta n_m^2 \mathbf{F}_k^*\cdot\mathbf{F}_m\,dxdy \\
&\qquad = i\omega_0 e^{-i(\beta_{0m}z-\omega_0 t)}\int\int_{-\infty}^{+\infty}\mathbf{F}_k^*\cdot\boldsymbol{P}^{(3)}dxdy.
\end{aligned} \tag{3.57}$$

The slowly varying third-order dipole-moment density $\boldsymbol{P}^{(3)}$ in Eq. (3.52) is related with the electric slowly varying amplitude $\boldsymbol{E}$. For simplicity, $\boldsymbol{P}^{(3)}$ can be approximately written as[9,14]

---

[9] G. P. Agrawal, *Nonlinear Fiber Optics,* 5th ed. (Academic Press, 2013).

[14] G. P. Agrawal, "Nonlinear fiber optics: its history and recent progress [invited]," J. Opt. Soc. Am. B 28, A1- A10 (2011).

$$\boldsymbol{P}^{(3)}(\mathbf{r},t)=\frac{3}{4}\varepsilon_0\chi^{(3)}_{xxxx}\boldsymbol{E}(\mathbf{r},t)\boldsymbol{E}^{*}(\mathbf{r},t)\boldsymbol{E}(\mathbf{r},t). \tag{3.58}$$

The real parameter $\chi^{(3)}_{xxxx}$ is related with n and nonlinear-index coefficient by: $\chi^{(3)}_{xxxx}=4\varepsilon_0 cn^2 n_2/3$. Here we are considering that the electronic response of the bound electrons in the silica atoms is extremely fast and can be taken to be instantaneous[9]. In addition, in Eq. (3.58) we are not considering the effect of third-harmonic frequency because this requires phase matching and it is generally negligible in optical fibers[9]. The electric slowly varying amplitude $\boldsymbol{E}$ in the time domain is given by

$$\boldsymbol{E}(\mathbf{r},t)=\sum_{m=1}^{2}A_m(z,t)\mathbf{F}_m(x,y)e^{i(\beta_{0m}z-\omega_0 t)}. \tag{3.59}$$

Substituting Eq. (3.59) into (3.58), and using the latter in Eq. (3.57), we obtain the following equation for the modal amplitudes:

$$\begin{aligned}\sum_{m=1}^{2}\left(\partial_z A_m-\sum_{n=1}^{\infty}i^{n+1}\frac{\beta_{nm}}{n!}\partial_t^n A_m\right)\frac{1}{\sqrt{N_m N_k}}\int\int_{-\infty}^{+\infty}(\mathbf{e}_m\times\mathbf{h}_k^{*}+\mathbf{e}_k^{*}\times\mathbf{h}_m)\cdot\hat{\mathbf{z}}\,dxdy\\ =i\omega_0\varepsilon_0\sum_{m=1}^{2}A_m\int\int_{-\infty}^{+\infty}\Delta n_m^2\mathbf{F}_k^{*}\cdot\mathbf{F}_m\,dxdy\\ +i\frac{3}{4}\varepsilon_0\omega_0\sum_{hnl}A_h A_n^{*}A_l\int\int_{-\infty}^{+\infty}\chi^{(3)}_{xxxx}(\mathbf{F}_h\cdot\mathbf{F}_n^{*})(\mathbf{F}_k^{*}\cdot\mathbf{F}_l)\,dxdy,\end{aligned} \tag{3.60}$$

[9] G. P. Agrawal, *Nonlinear Fiber Optics,* 5th ed. (Academic Press, 2013).

where the indices k, h, n, and l take values 1 to 2 that correspond to the modes of every fiber core that form the NLDFC. A compact form of Eq. (3.60) is given by

$$\sum_{m=1}^{2}\left(\partial_z A_m - \sum_{n=1}^{\infty} i^{n+1}\frac{\beta_{nm}}{n!}\partial_t^n A_m\right)\frac{1}{\sqrt{N_m N_k}}\int\int_{-\infty}^{+\infty}(\mathbf{e}_m\times\mathbf{h}_k^* + \mathbf{e}_k^*\times\mathbf{h}_m)\cdot\hat{\mathbf{z}}\,dxdy = 4i\sum_{m=1}^{2}\kappa_{km}A_m + 4i\sum_{hnl}\gamma_{hnl}^{(k)}A_h A_n^* A_l, \tag{3.61}$$

where

$$\kappa_{km} = \frac{\omega_0\varepsilon_0}{4\sqrt{N_k N_m}}\int\int_{-\infty}^{+\infty}\Delta n_m^2\,\mathbf{e}_k^*\cdot\mathbf{e}_m\,dxdy, \tag{3.62}$$

$$\gamma_{hnl}^{(k)} = \frac{\omega_0\bar{n}_2}{c\bar{A}_{eff}}. \tag{3.63}$$

κ_{km} is the coupling coefficient and $\gamma_{hnl}^{(k)}$ is the nonlinear parameter of the NLDFC. The additional parameters are given by

$$\bar{A}_{eff} = \left(\prod_{v=k,h,n,l} A_{eff}^{(v)}\right)^{1/4}, \tag{3.64}$$

$$A_{eff}^{(v)} = \frac{\left|\int\int_{-\infty}^{+\infty}(\mathbf{e}_v\times\mathbf{h}_v^*)\cdot\hat{\mathbf{z}}\,dxdy\right|^2}{\int\int_{-\infty}^{+\infty}\left|(\mathbf{e}_v\times\mathbf{h}_v^*)\cdot\hat{\mathbf{z}}\right|^2 dxdy}, \tag{3.65}$$

$$\bar{n}_2 = \left(\frac{\varepsilon_0}{\mu_0}\right)\frac{\int\int_{-\infty}^{+\infty} n^2(x,y)n_2(x,y)(\mathbf{e}_h\cdot\mathbf{e}_n^*)(\mathbf{e}_k^*\cdot\mathbf{e}_l)dxdy}{\left(\prod_{v=k,h,n,l}\int\int_{-\infty}^{+\infty}\left|(\mathbf{e}_v\times\mathbf{h}_v^*)\cdot\hat{\mathbf{z}}\right|^2 dxdy\right)^{1/4}}. \tag{3.66}$$

Equation (3.61) is a general relation that govern the behavior of the modal amplitudes of light pulses in a NLDFC. With the replacement of Eq. (3.35), Eq. (3.61) becomes

$$\begin{aligned}\partial_z A_k - \sum_{n=1}^{\infty} i^{n+1}\frac{\beta_{nk}}{n!}\partial_t^n A_k + \left(\partial_z A_m - \sum_{n=1}^{\infty} i^{n+1}\frac{\beta_{nm}}{n!}\partial_t^n A_m\right)\frac{C_{km}}{\sqrt{N_m N_k}} \\ = i\kappa_{kk}A_k + i\kappa_{km}A_m + i\sum_{hnl}\gamma_{hnl}^{(k)}A_h A_n^* A_l,\end{aligned} \tag{3.67}$$

where $k \neq m$ and k = 1,2. Although Eq. (3.67) appears complicated, it can be simplified in some specific situations. For example, if the NLDFC cores are identical, the coupling coefficients between both NLDFC cores are equal, i.e., $\kappa_{12} = \kappa_{21} = \kappa$ and $\kappa_{11} = \kappa_{22} = \kappa_2$. In addition, if the two NLDFC cores are sufficiently separated, κ_2 is much smaller than κ, and κ_2, C_{12}, and C_{21} can be neglected[4-5]. Alternatively, if the perturbation of the electric field amplitude A_2 inside the NLDFC core 1 is quite small when it is compared to its intensity $|A_2|^2$ or A_2^2, and similarly with A_1, then only four of the eight terms in the sum over h, n, l in Eq. (3.67), with k =1 or 2, are not vanishing. Therefore, the coupled mode equations are given by

[4] K. Okamoto, *Fundamentals of Optical Waveguides*, 2nd ed. (Academic Press, 2006).
[5] W. Snyder and J. D. Love, *Optical Waveguide Theory* (Kluwer Academic, 2000).

$$\partial_z A_1 - \sum_{n=1}^{\infty} i^{n+1} \frac{\beta_{n1}}{n!} \partial_t^n A_1 = i\kappa_1 A_2 + i\gamma_{111}^{(1)} |A_1|^2 A_1 + i2\gamma_{122}^{(1)} |A_2|^2 A_1 + i\gamma_{212}^{(1)} A_2^2 A_1^*, \quad (3.68)$$

$$\partial_z A_2 - \sum_{n=1}^{\infty} i^{n+1} \frac{\beta_{n2}}{n!} \partial_t^n A_2 = i\kappa_1 A_1 + i\gamma_{222}^{(2)} |A_2|^2 A_2 + i2\gamma_{211}^{(2)} |A_1|^2 A_2 + i\gamma_{121}^{(2)} A_1^2 A_2^*, \quad (3.69)$$

where $\gamma_{122}^{(1)} = \gamma_{221}^{(1)}$ and $\gamma_{211}^{(2)} = \gamma_{112}^{(2)}$.

In obtaining Eq. (3.68) and (3.69), we have used the normalization of each guided mode in the NLDFC given by[4 – 5]

$$\frac{1}{2}\int\int_{-\infty}^{+\infty} (\mathbf{e}_m \times \mathbf{h}_m^*) \cdot \hat{\mathbf{z}} dxdy = \frac{1}{2}\int\int_{-\infty}^{+\infty} (\mathbf{e}_m^* \times \mathbf{h}_m) \cdot \hat{\mathbf{z}} dxdy = N_m. \quad (3.70)$$

In Eq. (3.68) and (3.69), the parameters $\gamma_{111}^{(1)}$ and $\gamma_{222}^{(2)}$ are responsible for SPM, while the effects of XPM are governed by $\gamma_{122}^{(1)}$ and $\gamma_{211}^{(2)}$. Because we are considering a symmetric NLDFC with two identical fiber cores, we can define $\gamma_{111}^{(1)} = \gamma_{222}^{(2)} = \gamma$, $\gamma_{122}^{(1)} = \gamma_{211}^{(2)} = \gamma\sigma/2$, and $\gamma_{212}^{(1)} = \gamma_{121}^{(2)} = \eta$. Therefore,

$$\partial_z A_1 + i\frac{\beta_2}{2} \partial_T^2 A_1 = i\kappa_1 A_2 + i\gamma(|A_1|^2 + \sigma|A_2|^2) A_1 + i\eta A_2^2 A_1^*, \quad (3.71)$$

$$\partial_z A_2 + i\frac{\beta_2}{2} \partial_T^2 A_2 = i\kappa_1 A_1 + i\gamma(|A_2|^2 + \sigma|A_1|^2) A_2 + i\eta A_1^2 A_2^*, \quad (3.72)$$

[4] K. Okamoto, *Fundamentals of Optical Waveguides*, 2nd ed. (Academic Press, 2006).
[5] W. Snyder and J. D. Love, *Optical Waveguide Theory* (Kluwer Academic, 2000).

where we have retaining terms up to second order for $\beta_m(\omega)$. The time $T = t - z/v_g$ is measured in a frame of reference moving with the optical pulse at the group velocity v_g.

References

[1] G. P. Agrawal, *Applications of Nonlinear Fiber Optics*, 2nd ed. (Academic Press, 2008).

[2] M. Born and E. Wolf, *Principles of Optics*, 7th ed. (Cambridge University Press, 1999).

[3] A. Yariv and P. Yeh, *Photonics: Optical Electronics in Modern Communications*, 6th ed. (Oxford University Press, 2007).

[4] K. Okamoto, *Fundamentals of Optical Waveguides*, 2nd ed. (Academic Press, 2006).

[5] A. W. Snyder and J. D. Love, *Optical Waveguide Theory* (Kluwer Academic, 2000).

[6] Y. R. Shen, *Principles of Nonlinear Optics* (John Wiley & Sons, 1984).

[7] P. N. Butcher and D. N. Cotter, *The Elements of Nonlinear Optics* (Cambridge University Press, 1990).

[8] R. W. Boyd, *Nonlinear Optics,* 3rd ed. (Academic Press, 2008).

[9] G. P. Agrawal, *Nonlinear Fiber Optics,* 5th ed. (Academic Press, 2013).

[10] A. D. Bresler, G. H. Joshi, and N. Marcuvitz, "Orthogonality properties for modes in passive and active uniform wave guides," J. Appl. Phys **29**, 794-799 (1958).

[11] B. A. Daniel, D. N. Maywar, and G. P. Agrawal, "Dynamic mode theory of optical resonators undergoing refractive index changes," J. Opt. Soc. Am. B **28**, 2207-2215 (2011).

[12] A. Ghatak and K. Thyagarajan, Introduction to fiber optics (Cambridge University Press, 1997).

[13] C. Vassallo, *Optical Waveguide Concepts* (Elsevier, 1991).

[14] G. P. Agrawal, "Nonlinear fiber optics: its history and recent progress [invited]," J. Opt. Soc. Am. B **28**, A1-A10 (2011).

Chapter 4

Exact Analytical Solution of the Dispersionless Nonlinear Directional Fiber Coupler

Abstract

In this chapter, we develop for the first time, to the best of our knowledge, a comprehensive theory to describe the nonlinear propagation of picosecond pulses through symmetric NLDFCs. Considering the elementary NLDFC switching process, we have derived an exact analytical expression for the optical power and nonlinear phase shift of a picosecond pulse of arbitrary shape and chirp. Applying our results to a Gaussian input pulse, we have shown how the maximum nonlinear phase shift is affected by the linear coupling. To analyze this result, we have defined a critical coupling coefficient that determines the separation of the NLDFC cores at which the pulse energy is maximally exchanged from one NLDFC core to the other for the first time.

We also have shown that the critical coupling coefficient plays an important role in the NLDFC performance and has a dramatic impact on the accumulated nonlinear phase shift. In Section 4.1, we briefly introduce the way to solve the nonlinear coupled-mode equations that describe the NLDFC. In Section 4.2, we provide the analytical solution of the nonlinear coupled-mode equations. In addition, we give the analysis of the solution for the nonlinear phase shift and power that an optical pulse obtains in each NLDFC core. Finally, in Section 4.3 we give the analytical calculations of the output nonlinear phase shift and power in each NLDFC core.

4.1 Introduction

In general, exact analytical solutions to the coupled-mode Schrödinger equations for the NLDFC do not exist[1]. Therefore, approximations based on numerical methods are needed in order to solve the approximate scalar form of these equations. The split-step Fourier method is the common numerical method used to solve the coupled-mode Schrödinger equations[1]. However, because we are interested in the analysis of the nonlinear effects alone, we can neglect the dispersion effects in the NLDFC considering the propagation of picosecond pulses, and solve analytically the resulting equations. In this section, we solve analytically the nonlinear coupled-mode equations that describe the propagation of picosecond pulses along a lossless NLDFC. With the obtained analytical solutions of the power and nonlinear phase shift in each NLDFC core, we accurately analyze and obtain a physical insight of the effects of the linear coupling on the properties of the output signal pulses.

[1] G. P. Agrawal, *Applications of Nonlinear Fiber Optics* (Academic Press, 2008).

4.2 Nonlinear coupled-mode equations and their analytic solution

We begin by considering a lossless NLDFC with identical fiber cores of radius a, separated by a distance d between their centers, as shown in Fig. 4.1. More specifically, the NLDFC consist of a launch fiber core coupled with an unlaunch fiber core. The launch fiber core is a fiber core that is initially pumped with an optical pulse and the unlaunch fiber core is not initially pumped. Here we are considering the simplest situation in which a single-input pulse is launched into one NLDFC core such that it excites a single TE polarization mode of the NLDFC core. We can introduce the dispersion length in the usual way as $L_D = T_0^2/|\beta_2|$, where T_0 is the pulse width and β_2 is the GVD parameter[2].

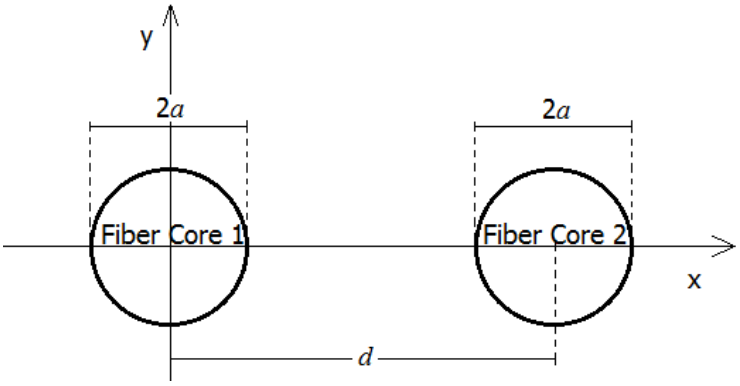

Fig. 4.1 Geometry of the symmetric NLDFC.

In Section 3.4, we obtained the coupled-mode Schrödinger equations that govern the propagation of optical pulses inside a NLDFC. For optical

[2] G. P. Agrawal, *Nonlinear Fiber Optics,* 5th ed. (Academic Press, 2013).

pulses, wide enough that L_D is much larger than the NLDFC length L, one can use Eqs. (3.71) and (3.72) and obtain

$$\partial_z A_1 + \frac{\alpha_1}{2} A_1 = i\kappa A_2 + i\gamma(|A_1|^2 + \sigma|A_2|^2)A_1, \tag{4.1}$$

$$\partial_z A_2 + \frac{\alpha_2}{2} A_2 = i\kappa A_1 + i\gamma(|A_2|^2 + \sigma|A_1|^2)A_2, \tag{4.2}$$

where we have neglected the last term in both equations. In addition, we have heuristically added the terms α_1 and α_2 to account the loss or gain in the corresponding NLDFC cores. Introducing the normalized amplitudes $U_m(z,T) = A_m(z,T)\exp(\alpha_m z/2)/\sqrt{P_0}$, where P_0 is the peak power of the incident pulse, Eqs. (4.1) and (4.2) become

$$\partial_z U_1 = i\kappa U_2 e^{-M_1 z/2} + i\frac{e^{-\alpha_1 z}}{L_{NL}}(|U_1|^2 + \sigma|U_2|^2 e^{-M_1 z})U_1, \tag{4.3}$$

$$\partial_z U_2 = i\kappa U_1 e^{+M_1 z/2} + i\frac{e^{-\alpha_2 z}}{L_{NL}}(|U_2|^2 + \sigma|U_1|^2 e^{+M_1 z})U_2, \tag{4.4}$$

where $M_1 = \alpha_2 - \alpha_1$ and $L_{NL} = (\gamma P_0)^{-1}$ is the nonlinear length. If $\alpha_m > 0$, the mth NLDFC core represents a lossy fiber core, but if $\alpha_m < 0$, the mth NLDFC core represents an active fiber core. Remember that we are considering the fundamental modes in the NLDFC are perfectly matched. The coupling coefficient κ and the cross-phase modulation (XPM) parameter σ, which represent the linear and nonlinear coupling coefficients respectively, depend on the distance d between the two NLDFC cores.

The complex slowly varying amplitude $U_m(z,T)$ of the mth NLDFC core has an instantaneous optical power of $P_m(z,T)=|U_m(z,T)|^2$. Both optical powers, $P_1(z,T)$ and $P_2(z,T)$, can vary along L because of the overlap of the two modes. Here it is convenient to define $P_{\pm}(z,T)=[P_1(z,T)\pm P_2(z,T)]/2$ such that $P_m(z,T)=[P_+(z,T)-(-1)^m P_-(z,T)]$.

We analytically solve Eqs. (4.3) and (4.4) by using a generalization of the well-known technique of introducing real amplitudes and phases terms $U_m(z,T)=\sqrt{P_m(z,T)}\exp\{i[\phi_{NLm}(z,T)+\phi_{0m}(0,T)]\}$. We note that $P_+(z,T)$ is a z constant $[P_+(z,T)/dz=0]$, so

$$U_m(z,T)=\sqrt{P_+(0,T)}\left[1-(-1)^m\frac{P_-(z,T)}{P_+(z,T)}\right]^{1/2}\exp\{i[\phi_{NLm}(z,T)+\phi_{0m}(0,T)]\},\quad(4.5)$$

where $\phi_{0m}(0,T)$ is a z constant, as well. Here we consider the specific case in which all the input power is initially launched into one NLDFC core (i.e., $U_2(0,T)=0$ at any time), therefore

$$U_1(z,T)=\frac{U_1(0,T)}{\sqrt{2}}\sqrt{1+u(z,T)}\exp[i\phi_1(z,T)],\quad(4.6)$$

$$U_2(z,T)=i\frac{U_1(0,T)}{\sqrt{2}}\sqrt{1-u(z,T)}\exp[i\phi_2(z,T)],\quad(4.7)$$

where $\phi_m(z,T)=\phi_{NLm}(z,T)+\phi_{0m}(0,T)$ and $u(z,T)=P_-(z,T)/P_+(z,T)$. $U_1(z,T)$ and $U_1(z,T)$ give the information of the behavior of the optical pulse when it

propagates through the launch and unlaunch NLDFC core, respectively. The factor i in Eq. (4.7) appears because the NLDFC introduces a relative phase shift of $\pi/2$ before any power is transferred to the second NLDFC core[1,3]. Initial conditions are such that $u(0,T)=1$, $\phi_1(0,T)=0$, and $\phi_2(0,T)=0$, for each time element. By inserting the solution from Eqs. (4.6) and (4.7) into Eqs. (4.3) and (4.4), we arrive at

$$\frac{du}{dz} = -2\kappa\sqrt{1-u^2}\cos\phi, \tag{4.8}$$

$$\frac{d\phi}{dz} = -\frac{2\kappa u}{\sqrt{1-u^2}}\sin\phi + \frac{|U_1(0,T)|^2}{L_{NL}}(\sigma-1)u, \tag{4.9}$$

where $\alpha_1 = \alpha_2 = 0$ and $\phi(z,T) = \phi_2(z,T) - \phi_1(z,T)$, and

$$\frac{d\phi_1}{dz} = -\frac{1-u}{\sqrt{1-u^2}}\kappa\sin\phi + \frac{|U_1(0,T)|^2}{2L_{NL}}[(\sigma+1)-(\sigma-1)u], \tag{4.10}$$

$$\frac{d\phi_2}{dz} = -\frac{1+u}{\sqrt{1-u^2}}\kappa\sin\phi + \frac{|U_1(0,T)|^2}{2L_{NL}}[(\sigma+1)+(\sigma-1)u]. \tag{4.11}$$

Equations (4.8) and (4.9) can be integrated using elliptic integrals[4]. Two kind of solutions of Eqs. (4.8) and (4.9), that satisfy the initial conditions, are available.

---

[1] G. P. Agrawal, *Applications of Nonlinear Fiber Optics* (Academic Press, 2008).

[3] C.-L. Chen, *Foundations for Guided-Wave Optics* (John Wiley and Sons, 2007).

[4] M. Abramowitz and I. A. Stegam, *Handbook of Mathematical Functions with Formulas, Graphs, and Mathematical Tables* (Dover, New York, 1972).

Solution 1:

$$u(z,T) = \mathrm{dn}\left(\frac{2\kappa z}{\sqrt{m_1}}\middle| m_1\right), \tag{4.12}$$

$$\phi(z,T) = \arccos\left[\mathrm{cn}\left(\frac{2\kappa z}{\sqrt{m_1}}\middle| m_1\right)\right]. \tag{4.13}$$

Solution 2:

$$u(z,T) = \mathrm{cn}(2\kappa z|m_2), \tag{4.14}$$

$$\phi(z,T) = \arccos[\mathrm{dn}(2\kappa z|m_2)]. \tag{4.15}$$

The Jacobi elliptic functions, $\mathrm{dn}(x_m|m_m)$ and $\mathrm{cn}(x_m|m_m)$, are two variable functions with argument x_m and modulus m_m. In our case, $m_1(T) = \left[4\kappa L_{NL}/(\sigma-1)|U_1(0,T)|^2\right]^2$ and $m_2(T) = \left[(\sigma-1)|U_1(0,T)|^2/4\kappa L_{NL}\right]^2$ are time-dependent parameters. Note that $m_1 = 1/m_2$.

The values of κ and P_0 for which $m_1 = 1$ and $m_2 = 1$ are defined as the critical coupling coefficient κ_c and critical power P_c, respectively. The substitution of solution 1 or 2 into Eq. (4.9) produces the function $f(\kappa)$ (when $m_1 = 1$ or $m_2 = 1$):

$$f(\kappa) = 4\kappa L_{NL} - [1-\sigma(\kappa)]|U_1(0,T)|^2. \tag{4.16}$$

κ_c is the solution of the function $f(\kappa)=0$. This is so because σ depends on κ in general. By using the definition of L_{NL}, P_c is given by

$$P_c = \frac{4\kappa_c}{\gamma[1-\sigma(\kappa_c)]|U_1(0,T)|^2} = \frac{4\kappa_c}{\gamma[1-\sigma(\kappa_c)]P_1(0,T)}. \tag{4.17}$$

For any elliptic function, its modulus must lie between 0 and 1. Using the condition $0 \le m_1 \le 1$ or $0 \le m_2 \le 1$, we obtain

$$\frac{\kappa}{P_0} \le \frac{\gamma}{4}(1-\sigma)|U_1(0,T)|^2 = \frac{\kappa_c}{P_c}, \tag{4.18}$$

or

$$\frac{\kappa}{P_0} \ge \frac{\gamma}{4}(1-\sigma)|U_1(0,T)|^2 = \frac{\kappa_c}{P_c}, \tag{4.19}$$

respectively.

Equation (4.17) reduces to the well-known definition of the continuous wave P_c ($|U_1(0,T)|^2=1$)[1,5]. In the case of optical pulses, both κ_c and P_c are time-dependent functions that give rise to a power-dependent transmission and a pulse intensity discrimination[6]. These two parameters play an important role because they define a boundary between the two possible solutions (solutions 1 and 2) of Eqs. (4.8) and (4.9). It is important to note [Eqs. (4.16) and (4.17)] that γ controls the relationship between κ_c and P_c.

---

[1] G. P. Agrawal, *Applications of Nonlinear Fiber Optics* (Academic Press, 2008).

[5] S. M. Jensen, "The nonlinear coherent coupler," IEEE J. Quantum Electron. **QE-18**, 1580-1583 (1982).

[6] E. E. Nazemosadat and A. Mafi, "Saturable absorption in multicore fiber couplers," J. Opt. Soc. Am. B **30**, 2787-2790 (2013).

In general, solutions 1 and 2 form a complete solution of the system for all values of κ and P_0. Equation (4.18) shows that solution 1 applies when $0 < \kappa \leq \kappa_c$ or/and the input power is high ($P_c \leq P_0 < \infty$); resulting into a reduction in the power exchange efficiency, i.e., the linear coupling effect is reduced and the optical field remains primarily in the launch NLDFC core. On the other hand, Eq. (4.19) shows that solution 2 applies when $\kappa_c \leq \kappa < \infty$ or/and the input power is low ($0 < P_0 \leq P_c$). It is well-known that in this case, both $P_1(z,T)$ and $P_2(z,T)$ vary sinusoidally with z for any directional coupler[1,3,7]. The periodic power transfer between the two NLDFC cores depends on the parameter κL. In particular, L_c is the shortest distance coupling length at which the maximum power is transferred to the second NLDFC core for the first time.

The parameter that defines the boundary between the low-power and high-power regimes is P_c. Analogously, it is easy to show that the parameter that defines the boundary between the weak-coupling ($0 < \kappa \leq \kappa_c$) and strong-coupling ($\kappa_c \leq \kappa < \infty$) regimes is κ_c. In particular, κ_c acts as the overlap enhancement starting point of the fields associated with the two NLDFC cores. NLDFCs can thus operate in two distinct regimes:

---

[1] G. P. Agrawal, *Applications of Nonlinear Fiber Optics* (Academic Press, 2008).

[3] C.-L. Chen, *Foundations for Guided-Wave Optics* (John Wiley and Sons, 2007).

[7] K. Okamoto, Fundamentals of Optical Waveguides (Academic Press, New York, 2000)

4.2.1 Nonlinear Regime

In this regime, κ and P_0 satisfy the following inequalities: $0 < \kappa \leq \kappa_c$ and $P_c \leq P_0 < \infty$. For this case, we demonstrate below that the evanescent field is so weak that we can neglect both the XPM effect (negligible σ) and the field transfer among the NLDFC cores. Here the expressions for the output powers are given by

$$P_1(L,T) = \frac{|U_1(0,T)|^2}{2}\left[1 + \mathrm{dn}\left(\frac{L}{2L_{NL}}|U_1(0,T)|^2(\sigma - 1)\middle| m_1\right)\right], \tag{4.20}$$

$$P_2(L,T) = \frac{|U_1(0,T)|^2}{2}\left[1 - \mathrm{dn}\left(\frac{L}{2L_{NL}}|U_1(0,T)|^2(\sigma - 1)\middle| m_1\right)\right]. \tag{4.21}$$

Using Eqs. (4.20) and (4.21), we can notice that $P_{-}(L,T) \geq 0$ because the function $0 \leq \mathrm{dn}(x_1 \mid m_1) \leq 1$. Therefore, as light propagates in the NLDFC, the total power in the launch NLDFC core cannot be transferred to the other NLDFC core. Therein, the XPM effect is so small that we can neglect σ. Using Eqs. (4.12) and (4.13) to integrate Eqs. (4.10) and (4.11), we obtain the output nonlinear phases in this regime that are given by

$$\begin{aligned}\phi_{NL1}(L,T) = {} & \frac{L}{4L_{NL}}|U_1(0,T)|^2(\sigma + 3) \\ & - \frac{(-1)^{k_1}}{2}\arcsin\left\{\mathrm{sn}\left[\frac{L}{2L_{NL}}|U_1(0,T)|^2(\sigma - 1)\middle| m_1\right]\right\} - \frac{\pi k_1}{2},\end{aligned} \tag{4.22}$$

$$\phi_{NL2}(L,T) = \frac{L}{4L_{NL}}\left|U_1(0,T)\right|^2(\sigma+3) + \frac{(-1)^{k_1}}{2}\arcsin\left\{\mathrm{sn}\left[\frac{L}{2L_{NL}}\left|U_1(0,T)\right|^2(\sigma-1)\middle| m_1\right]\right\} + \frac{\pi k_1}{2}, \tag{4.23}$$

where k_1 is defined by the argument and period of the Jacobian elliptic function $\mathrm{sn}(x_1|m_1)$. More specifically, k_1 is an integer given by

$$k_1 = \left\| \frac{L(2L_{NL})^{-1}\left|U_1(0,T)\right|^2(\sigma-1)}{2K_1} \right\|, \tag{4.24}$$

where $K_1(m_1)$ is a complete elliptic integral of the first kind. $\|x\|$ means the nearest integer to x.

Because we are in the regime in which κ can be so small but not zero or/and P_0 can be so high but not infinity, we are going to analyze what happen in the limit when we separate the two NLDFC cores or/and we launch a pulse with strong P_0 to the NLDFC such that any power from the launch NLDFC core cannot be transferred to the other NLDFC core. In this decoupling limit, when $\kappa \to 0$ ($\sigma \to 0$), or/and $P_0 \to \infty$, the modulus $m_1 \to 0$. Therefore, $\phi_{NL1}(L,T) \to \left|U_1(0,T)\right|^2 L/L_{NL}$ and $\phi_{NL2}(L,T) \to \left|U_1(0,T)\right|^2 L/(2L_{NL})$.

In this limit, we can see that $\phi_{NL1}(L,T)$ recovers the standard form obtained for SCFs. For a useful notation, we define these last two limiting values as: $\phi_{NL1}^{\kappa\to 0}(L,T) = \left|U_1(0,T)\right|^2 L/L_{NL}$ and $\phi_{NL2}^{\kappa\to 0}(L,T) = \phi_{NL1}^{\kappa\to 0}(L,T)/2$. In fact,

$\phi_{NL2}(L,T) = 0$ when $\kappa = 0$ because of the initial conditions, however, $\phi_{NL2}(L,T)$ reach the $\phi_{NL2}^{\kappa\to 0}(L,T)$ value because this is the nonlinear phase lowest value that can reach $\phi_{NL2}(L,T)$ when an exchange of power begins or ends. Here we define the maximum nonlinear phase shifts at the pulse center as $\phi_{max1} = \phi_{NL1}(L,0)$ and $\phi_{max2} = \phi_{NL2}(L,0)$, where the complex slowly varying amplitude of the input pulse is normalized such that $|U_1(0,0)| = 1$. Therefore, in the decoupling limit, $\phi_{max1}^{\kappa\to 0} = L/L_{NL}$ and $\phi_{max2}^{\kappa\to 0} = \phi_{max1}^{\kappa\to 0}/2$.

4.2.2 Linear Regime

In this regime, κ and P_0 satisfy the following inequalities: $\kappa_c \le \kappa < \infty$ and $0 < P_0 \le P_c$. For this case, we derive the expressions that govern the power exchange between both NLDFC cores. The expressions for the output powers are given by

$$P_1(z,T) = \frac{|U_1(0,T)|^2}{2}[1 + \mathrm{cn}(2\kappa L|m_2)], \tag{4.25}$$

$$P_2(z,T) = \frac{|U_1(0,T)|^2}{2}[1 - \mathrm{cn}(2\kappa L|m_2)]. \tag{4.26}$$

From Eqs. (4.25) and (4.26), we find that the coupling length is given by $L_c = K_2/\kappa$, where $K_2(m_2)$ is a complete elliptic integral of the first kind. Using Eqs. (4.14) and (4.15) to integrate Eqs. (4.10) and (4.11), we obtain the output nonlinear phases in this regime that are given by

$$\phi_{NL1}(L,T)=\frac{L}{4L_{NL}}\left|U_1(0,T)\right|^2(\sigma+3)-\frac{(-1)^{k_2}}{2}\arccos[\mathrm{dn}(2\kappa L|m_2)], \quad (4.27)$$

$$\phi_{NL2}(L,T)=\frac{L}{4L_{NL}}\left|U_1(0,T)\right|^2(\sigma+3)+\frac{(-1)^{k_2}}{2}\arccos[\mathrm{dn}(2\kappa L|m_2)], \quad (4.28)$$

where k_2 is an integer that depends on the argument and period of $\mathrm{dn}(x_2|m_2)$. More specifically, k_2 is given by

$$k_2=\left\|\frac{\kappa L}{K_2}-\frac{1}{2}\right\|. \quad (4.29)$$

In this regime, κ can be so large but not infinity or/and P_0 can be so low but not zero. We are going to analyze what happen in the limit when we put together the two NLDFC cores so close or/and we launch a pulse with low P_0 to the NLDFC such that an exchange of power between the two NLDFC cores is observed. In this coupling limit, when $\kappa\to\infty$ or/and $P_0\to 0$, the modulus $m_2\to 0$ and therefore $\phi_{NLm}(L,T)\to\left|U_1(0,T)\right|^2(3+\sigma)L/4L_{NL}$ and $L_c=\pi/2\kappa$, which is the standard definition of the coupling length of linear directional couplers. Assuming that $\sigma\approx 0$ when $d/a>4$, we define the last limit values as: $\phi_{NLm}^{\kappa\to\infty}(L,T)=3\phi_{NL1}^{\kappa\to 0}(L,T)/4$. Note that both nonlinear phases tend to the same value, i.e., when a NLDFC undergoes a strong linear coupling the output nonlinear phases will be the same, approximately.

As in the previous section, we define the maximum nonlinear phase shifts at the pulse center as $\phi_{max1} = \phi_{NL1}(L,0)$ and $\phi_{max2} = \phi_{NL2}(L,0)$, where the complex slowly varying amplitude of the input pulse is normalized such that $|U_1(0,0)| = 1$. Therefore, in the coupling limit $\phi_{max1}^{K\to\infty} = \phi_{max2}^{K\to\infty} = \frac{3}{4}L/L_{NL}$.

4.3 Analytical calculations of the output nonlinear phase shifts and powers

In this section, we graphically show how the nonlinear phase shifts and powers in a lossless NLDFC are affected by the linear coupling. For this task, we have considered the simplest case when a unchirped Gaussian pulse of the form

$$U_1(0,T) = \exp\left(-\frac{1}{2}\frac{T^2}{T_0^2}\right), \tag{4.30}$$

is launched into one NLDFC core.

Figure 4.2 shows the two distinctive NLDFC regimes by a calculation of the analytical solutions of the output powers and nonlinear phase shifts at the pulse center. We chose the following values for our calculations: $T_0 = 100\,\text{ps}$, $P_0 = 4\pi\,\text{W}$, $|\beta_2| = 20\,\text{ps}^2/\text{km}$, and $\gamma = 2\,\text{km}^{-1}\text{W}^{-1}$ at $\lambda = 1.55\,\mu\text{m}$. Therefore, we obtain that $L_D = 500\,\text{km}$ and $L_{NL} = 0.04\,\text{km}$. With these values, we ensure to minimize the dispersion effects in the NLDFC. Additional values are: $a = 4\,\mu\text{m}$,

the relative fiber core-cladding index difference $\Delta = 0.3\%$, the normalized frequency V=2 and L=1 km.

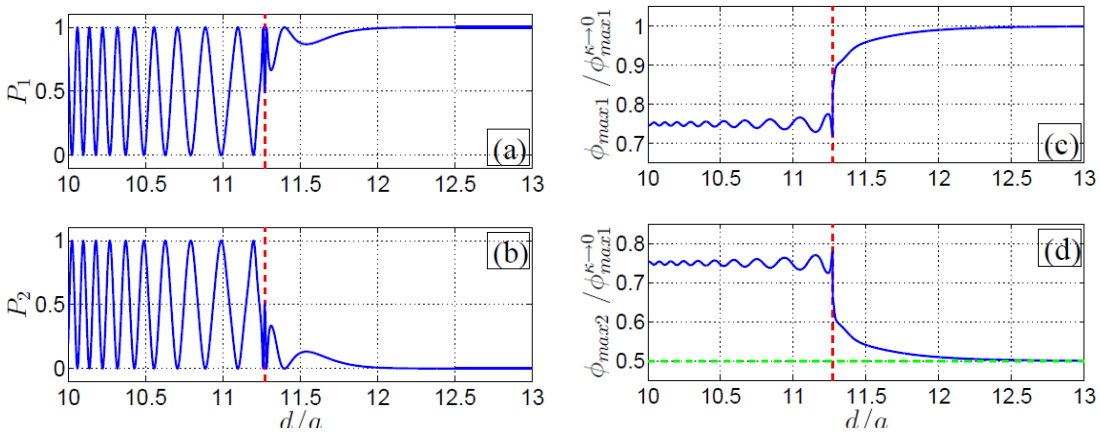

Fig. 4.2 The role of κ_c is shown in (a), (b), (c) and (d), and the drop of the NLPS is shown in (c) and (d). The output power and nonlinear phase at the pulse center, P_1 and $\phi_{max1}/\phi_{max1}^{\kappa\to\infty}$ at the upper, and P_2 and $\phi_{max2}/\phi_{max2}^{\kappa\to\infty}$ at the bottom of each figure, respectively. The d/a value related with the κ_c value has been marked down by a red dashed line that separates both NLDFC regimes.

We show the role of κ_c in the design of NLDFCs and the drop of the output nonlinear phase shift of the signal pulse when an interchange of power begins between the two NLDFC cores. Using the values of L and L_{NL} for our calculations, we obtain: $\phi_{max1}^{\kappa\to 0} = 8\pi$ and $\phi_{maxm}^{\kappa\to\infty} = 6\pi$. In this regard, there is a suppression of 2π in the normalized maximum nonlinear phase shift. For convenience, we have plotted our graphic (Fig. 4.2) in terms of d/a where it is clearly noticeable that the d/a value related with the κ_c value, marked

down by a red dashed line, separates both NLDFC regimens. The κ_c value displaces to the left when γ or P_0 is larger (see Eq. (4.17)). Notice that at κ_c, the growth in the linear coupling results into a smooth jump for both the output power and normalized maximum nonlinear phases in such way that a transfer of power between the two NLDFC cores begins and a second state of the nonlinear phase shift persists. Also, note that the nonlinear phase shift has a reduction only when all the power in the launch NLDFC core is transferred to the other NLDFC core, and although we are increasing the linear coupling the nonlinear phase shift will continue with the saturated value.

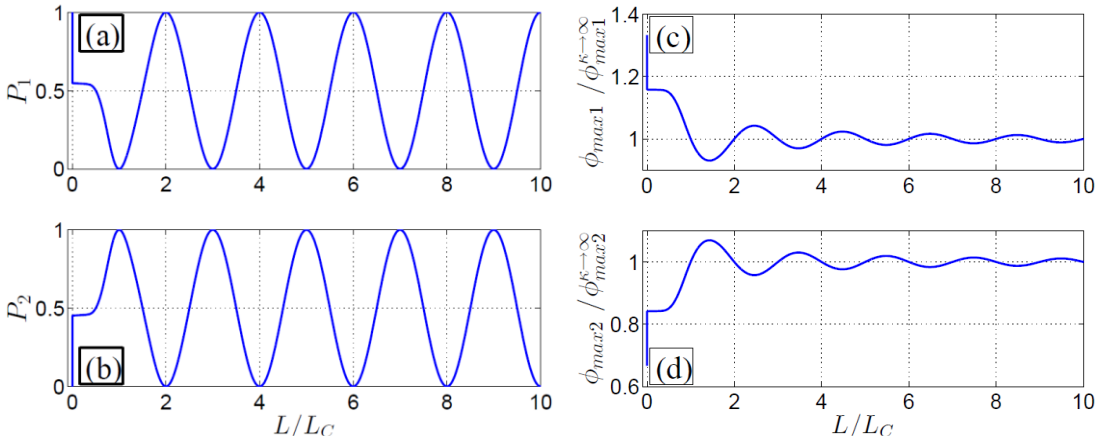

Fig. 4.3 The drop of the NLPS is shown in (c) and (d). The output power and nonlinear phase at the pulse center, P_1 and $\phi_{max1}/\phi_{max1}^{\kappa\to\infty}$ at the upper, and P_2 and $\phi_{max2}/\phi_{max2}^{\kappa\to\infty}$ at the bottom of each figure, respectively.

To analyze more carefully the system, we illustrate in Fig. 4.3 (see below) the analytical expressions of the output nonlinear phases and powers

at the pulse center in terms of L/L_c, where $L/L_c = (L/K_2)\kappa$. These results indicate that the output nonlinear phases reach a saturation value in such a way that $\phi_{maxm} \to \phi_{maxm}^{\kappa\to\infty}$ as L/L_c grows. The absolute state differences for each maximum nonlinear phase through the critical regions are given by: $\left|\phi_{maxm}^{\kappa\to 0} - \phi_{maxm}^{\kappa\to\infty}\right| = \phi_{max1}^{\kappa\to 0}/4$. These relations show that the nonlinear phase shift is reduced a quantity that depends on L, P_0, and γ, when a transfer of power between the two NLDFC cores begins. However, the total suppression of the nonlinear phase shifts with respect to $\phi_{max1}^{\kappa\to 0}$ is always a constant.

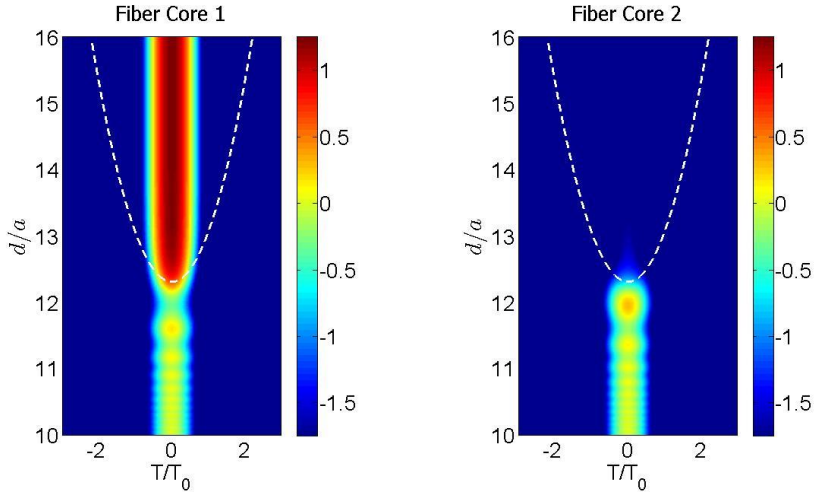

Fig. 4.4 Temporal variation of the normalized nonlinear phase shifts $\phi_{NL1}/\phi_{NL1}^{\kappa\to\infty}$ (left) and $\phi_{NL2}/\phi_{NL2}^{\kappa\to\infty}$ (right) as a function of d/a. The d/a values related with the κ_c values has been marked by a white dashed line that separates both NLDFC regimes. The color scale is logarithmic and represents the normalized nonlinear phase shift density on a 3 dB scale (see the color bar).

In Figs. 4.4 and 4.5, we depict again the two distinctive NLDFC regimes by a simulation of the analytical solutions of the powers and output nonlinear

phases of the whole pulse. We show the temporal variation of the normalized nonlinear phase shifts $\phi_{max1}/\phi_{max1}^{\kappa\to\infty}$ and $\phi_{max2}/\phi_{max2}^{\kappa\to\infty}$, and normalized output powers, P_1 and P_2, as a function of the relative core-center separation d/a.

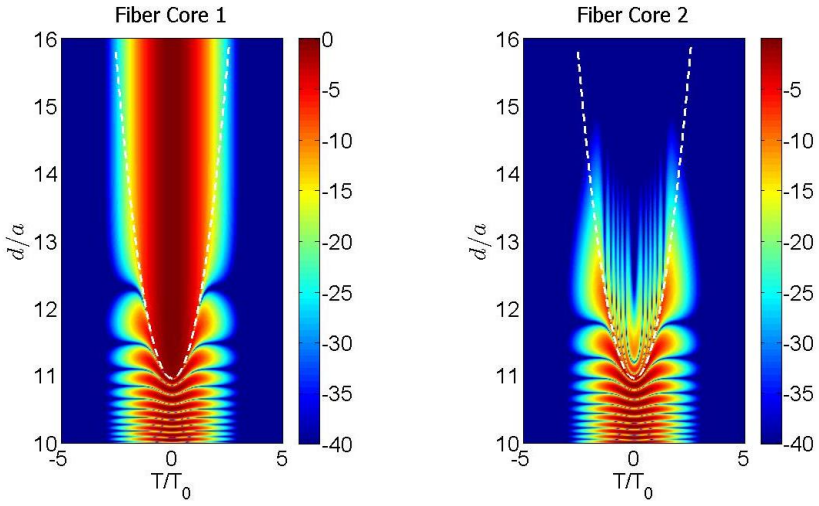

Fig. 4.5 Temporal variation of the normalized output powers P_1 (left) and P_2 (right) as a function of d/a. The d/a values related with the κ_c values has been marked by a white dashed line that separates both NLDFC regimes. The color scale is logarithmic and represents the power density on a 40 dB scale (see the color bar).

In summary, we derived an exact analytical expression for the nonlinear phase shift of an optical pulse propagating in a NLDFC with single-input excitation. Applying our results to an input Gaussian pulse, we showed that the nonlinear phase shift at the output is reduced and attains a saturation value when the joint effects of the linear and nonlinear couplings cause a quasi-periodic power transfer between the two NLDFC cores. This means that the simple interaction between the two NLDFC cores produces a reduction of the nonlinear phase shift through the first transmission of power from the

launch NLDFC core to the other NLDFC core. To analyze this result, we defined a critical coupling coefficient that determines the separation of the NLDFC cores at which the reduction in the nonlinear phase shift occurs. In addition, we found that the nonlinear phase shift is reduced in proportion with L, P_0, and γ.

References

[1] G. P. Agrawal, *Applications of Nonlinear Fiber Optics* (Academic Press, 2008).

[2] G. P. Agrawal, *Nonlinear Fiber Optics,* 5th ed. (Academic Press, 2013).

[3] C.-L. Chen, *Foundations for Guided-Wave Optics* (John Wiley and Sons, 2007).

[4] M. Abramowitz and I. A. Stegam, *Handbook of Mathematical Functions with Formulas, Graphs, and Mathematical Tables* (Dover, New York, 1972).

[5] S. M. Jensen, "The nonlinear coherent coupler," IEEE J. Quantum Electron. **QE-18**, 1580-1583 (1982).

[6] E. E. Nazemosadat and A. Mafi, "Saturable absorption in multicore fiber couplers," J. Opt. Soc. Am. B 30, 2787-2790 (2013).

[7] K. Okamoto, Fundamentals of Optical Waveguides (Academic Press, New York, 2000).

Chapter 5

Impact of Linear Coupling on Nonlinear Phase Noise in Nonlinear Directional Fiber Couplers

Abstract

In this chapter, we study the effect of the linear coupling on the nonlinear phase noise in NLDFCs when a single-input excitation is considered to perform optical switching. For this purpose, we use a Gaussian probability density function to represent the statistical properties of a stochastic continuous-wave optical power input. We show how the variance of the output nonlinear phase shift is reduced when the exchange of optical power begins between the two NLDFC cores. We also show that the signal-to-noise ration (SNR) of the output nonlinear phase shift is maximally improved just

when the linear coupling achieves L equals to one L_c or two L_c, i.e., when $L = nL_c$, with n = 1 or 2. Moreover, if n grows, the SNR tends to 0 and hence it is not improved by the linear coupling.

5.1 Nonlinear phase noise

Consider an optical signal launched into one NLDFC core immediately after its amplification by an in-line optical amplifier. The total electric field envelope after the amplifier can be expressed mathematically as follows:

$$U_1(0,T) = s_1(0,T) + n_1(0,T), \tag{5.1}$$

where $s_1(0,T)$ is the input signal field and $n_1(0,T)$ is the time-dependent noise field added by the amplifier due to spontaneous emission. Typically, $n_1(0,T)$ is much smaller than $s_1(0,T)$ at any time. As a result, the electric field envelope $U_1(0,T)$ is randomly varying in time, and its propagation through a NLDFC becomes a random process.

In general, the complex amplitude noise $n_1(0,T)$, which has both the in-phase and quadrature components, is a statistically independent and identically distributed Gaussian random variable with zero mean and variance $2\sigma_1^2$, where σ_1^2 is the noise variance per dimension[1]. Therefore, the time-dependent mean and variance of $|U_1(0,T)|^2$ are given by[2]

---

[1] K.-P. Ho, "Probability density of nonlinear phase noise," J. Opt. Soc. Am. B **20**(9), 1875–1879 (2003).

[2] K.-Po Ho and J. M. Kahn, "Electronic Compensation Technique to Mitigate Nonlinear Phase Noise," J. Lightwave Technol. **22**(3), 779–783 (2004).

$$m_{|U_1(0,T)|^2} = |s_1(0,T)|^2 + 2\sigma_1^2, \tag{5.2}$$

$$\sigma^2_{|U_1(0,T)|^2} = 4|s_1(0,T)|^2\sigma_1^2 + 4\sigma_1^4. \tag{5.3}$$

Considering the simplest case when a noisy CW beam ($|s_1(0,T)|^2 = 1$) is launched into one NLDFC core, therefore, the stochastic input signal power is given by

$$|U_1(0,T)|^2 = 1 + 2\sqrt{2}\sigma_1 + 2\sigma_1^2, \tag{5.4}$$

where σ_1 change according with a Gaussian distribution with time.

The overall output nonlinear phases of the NLDFC caused by the stochastic input signal $U_1(0,T)$ (Eq. (5.1)) are given by Eqs. (4.19) and (4.22). Using Eq. (5.4), we can investigate the effect of the linear coupling on the variances, $\sigma^2_{\phi_{NL1}}$ and $\sigma^2_{\phi_{NL2}}$, of the two output nonlinear phases, $\phi_{NL1}(L,T)$ and $\phi_{NL2}(L,T)$, respectively. In the limit when there is no coupling between the two NLDFC cores, $\sigma^2_{\phi_{NL1}} \to \sigma^2_{\phi_{NL}}$, where $\sigma^2_{\phi_{NL}}$ is the variance of the output NLPS, $\phi_{NL}(L,T) = |U_1(0,T)|^2 L/L_{NL}$, which corresponds to the same electromagnetic field propagating along a SCF that has the same physical properties like one NLDFC core.

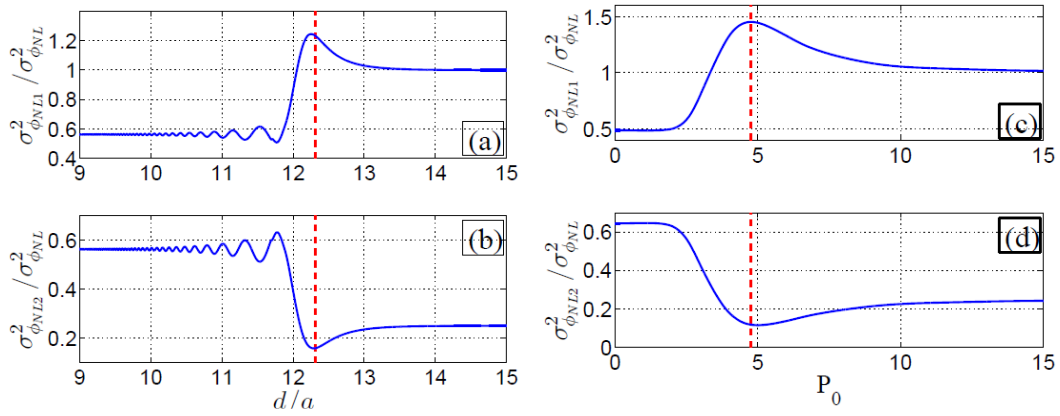

Fig. 5.1 Ratio of the variances, $\sigma^2_{\phi_{NL1}}$ and $\sigma^2_{\phi_{NL}}$, at the upper, and $\sigma^2_{\phi_{NL2}}$ and $\sigma^2_{\phi_{NL}}$, at the bottom of each figure, (a) and (b) versus the relative core center separation d/a and (c) and (d) versus P_0. (a) and (b) $P_0 = \pi$ W and (c) and (d) $d/a = 12$. The d/a and P_0 values related with the κ_c and P_c values, respectively, have been marked down by a red dashed line that separates both NLDFC regimens.

Figure 5.1 shows the ratios of the two independent estimates of variance, $\sigma^2_{\phi_{NL1}}$ and $\sigma^2_{\phi_{NL}}$, and $\sigma^2_{\phi_{NL2}}$ and $\sigma^2_{\phi_{NL}}$, as a function of the relative core center separation d/a, and as a function of P_0. We chose the following values for our calculations: L=1 km, $\gamma = 2\,\text{km}^{-1}\text{W}^{-1}$, and $\sigma_1^2 = 0.01$. Notice that the variance $\sigma^2_{\phi_{NL1}}$ undergoes a reduction of around of 42%, with respect to the variance of a SCF nonlinear phase shift, in its saturation value magnitude when the joint effects of the linear and nonlinear couplings or/and P_0 cause a periodic power transfer between the two NLDFC cores. This means that the simple interaction between the two NLDFC cores produces a reduction of the variance of the nonlinear phase shift through the first transmission of power from the launch NLDFC core to the other NLDFC core.

In other words, this is the origin of a suppression of the nonlinear phase noise of an optical beam propagating through the NLDFC. In Fig. 5.1(a) and (b), independently of the values of L, P_0, and γ, the reduction of $\sigma^2_{\phi_{NL1}}$ with respect to $\sigma^2_{\phi_{NL}}$ is always a contant. This is so because the total reduction of the nonlinear phase shift with respect to $\phi^{\kappa\to 0}_{NL1}$ is always a constant as well. The behavior of $\sigma^2_{\phi_{NL1}}$ and $\sigma^2_{\phi_{NL2}}$ follows the behavior of ϕ_{NL1} and ϕ_{NL2}. The peaks at κ_c and P_c in Fig. 5.1(a) and 5.1(c), respectively, are related with the degradation of the performance of the NLDFC because at these levels the nonlinear phase noise is maximized.

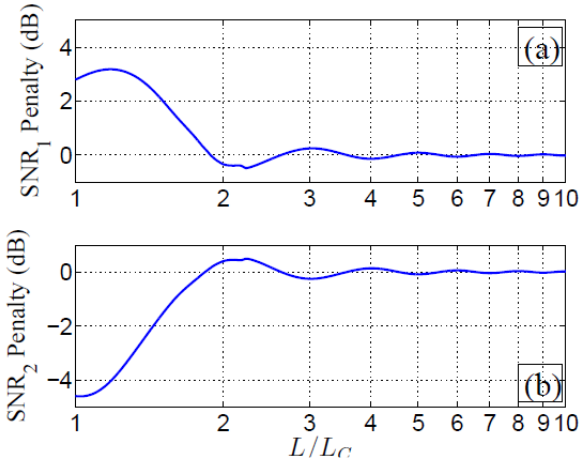

Fig. 5.2 Normalized SNR at the output of every NLDFC core, SNR_1/SNR_0 and SNR_2/SNR_0, in dB units, as a function of $L/L_c = (L/K_2)\kappa$.

In Fig. 5.2, we show the SNR penalties of the nonlinear phase shifts, at the output of every NLDFC core. $SNR_1\,\text{Penalty} = 10\log_{10}(SNR_0/SNR_1)$ and

SNR_2 Penalty$=10\log_{10}(SNR_0/SNR_2)$, where $SNR_1 = <\phi_{NL1}>^2/\sigma^2_{\phi_{NL1}}$ and $SNR_2 = <\phi_{NL2}>^2/\sigma^2_{\phi_{NL2}}$). The $SNR_0 = <\phi_{NL}>^2/\sigma^2_{\phi_{NL}}$) represents the SNR of a SCF nonlinear phase shift. In the plot, we can see that the NLDFC SNR at the output is maximally improved just when the linear coupling produce that $L = L_c$, when the optical signal is collected from the unlaunch fiber core, and also at $L = 2L_c$, when the optical signal is collected from the launch core. In other words, the SNR_2 penalty is negative (<0 dB) when the linear coupling produce that $L = L_c$. This indicates an improvement of the system performance caused by linear coupling in reference with the performance of a SCF. When $L = nL_c$, with n growing, the SNR tends to 0 and it is not improved by the linear coupling.

References

[1] K.-P. Ho, "Probability density of nonlinear phase noise," J. Opt. Soc. Am. B **20**(9), 1875–1879 (2003).

[2] K.-Po Ho and J. M. Kahn, "Electronic Compensation Technique to Mitigate Nonlinear Phase Noise," J. Lightwave Technol. **22**(3), 779–783 (2004).

Chapter 6

Compensation of Self-Phase Modulation through Linear Coupling in Nonlinear Directional Fiber Couplers

Abstract

In this chapter, we present the results of a theoretical study of the effect of linear coupling on the frequency spectrum of an initial unchirped optical pulse propagating through a NLDFC. We have focused on a NLDFC, which is the simplest, but most important, setup of MCFs to obtain physical insight of the effect of linear coupling on the phenomenon of SPM. For our purposes, the analysis of the elementary switching process in a NLDFC was suffice to obtain considerable and comprehensible results. We demonstrate spectral narrowing in the propagation of an initial unchirped optical pulse through a NLDFC. Our

results show that the linear coupling between both NLDFC cores induces that spectral narrowing. The amount of narrowing of the pulse spectra depend on the peak power of the input optical pulse. First in Section 6.1, we present an introduction of the nonlinear phenomenon of SPM in NLDFCs.

In Section 6.2 we graphically show how the linear coupling affect the power and SPM-induced phase shift of an optical pulse propagating through a NLDFC. For this purpose, we consider an unchirped Gaussian input pulse and the role of κ_c in describing NLDFCs.

6.1 Introduction

In SCFs, the nonlinear effect of SPM gives rise to an intensity-dependent phase shift called nonlinear phase shift[1]. The time dependence of the nonlinear phase shift caused by the temporal behavior of the amplitude function of an optical pulse induces spectral broadening[1]. On the positive side, SPM-induced spectral broadening plays an important role in many cases of light-wave propagation such as soliton formation and supercontinuum generation[1,2], and it is widely applied for all-optical regeneration[3]. On the negative side[4,5], it degrades the performance of high-bandwidth optical fiber communication systems, and it is a limiting factor in high-power fiber laser systems[6,7].

---

[1] G. P. Agrawal, *Nonlinear Fiber Optics,* 5th ed. (Academic Press, 2013).

[2] R. R. Alfano, *The Supercontinuum Laser Source*, 2nd ed. (Springer, 2006).

[3] P. V. Mamyshev, "All-optical data regeneration based on self-phase modulation effect," in Proc. European Conference on Optical Communications (ECOC'98), p. 475-476, 1998.

[4] R. H. Stolen and C. Lin, "Self-phase modulation in silica optical fibers," Phys. Rev. A **17**, 1448-1453 (1978).

[5] G. P. Agrawal, *Fiber-Optic Communication Systems*, 4th ed. (Wiley, 2010).

[6] W. J. Tomlinson, R. H. Stolen, and C. V. Shank, "Compression of optical pulses chirped by self-phase modulation in fibers," J. Opt. Soc. Am. B **1**, 139-149 (1984).

The SPM-induced phase shift and spectral broadening of an optical pulse propagating through a fiber core that is coupled with adjacent parallel fiber cores are still unexplored. This is due in part by the complexity of the systems of multiple fiber cores named MCFs. However, SPM-induced spectral broadening in MCFs plays the same important positive and negative role than in SCFs. In fact, it is very important for soliton switching[8,9] and multi-frequency generation[10,11] in MCF couplers. In addition, its understanding in MCFs results quite promising to optimize the engineering of novel components for information technology such as mode-locked MCF lasers, and MCF amplifiers.

6.2 Impact of Linear Coupling on Self-Phase Modulation of Optical Pulses in a NLDFC

In Chapter 4, we have showed how the linear coupling affects the maximum nonlinear phase shift of an optical pulse after propagating through the length of a NLDFC. $\phi_{NL1}(L,T)$ gives the form of the output nonlinear phase shift when the optical pulse leaves the launch NLDFC core at the output, and $\phi_{NL2}(L,T)$ gives the form when the optical pulse leaves the unlaunch NLDFC core at the output. The effect of linear coupling on SPM in a NLDFC can be

---

7 J. van Howe, G. Zhu, and C. Xu, "Compensation of self-phase modulation in fiber-based chirped-pulse amplification systems," Opt. Lett. **31**, 1756-1758 (2006).

8 Y. S. Kivshar and M. L. Quiroga-Teixeiro, "Influence of cross-phase modulation on soliton switching in nonlinear optical fibers," Opt. Lett. **18**, 980-982 (1993).

9 P. L. Chu, Y. S. Kivshar, B. A. Malomed, G.-D. Peng, and M. L. Quiroga-Teixeiro, "Soliton controling, switching, and splitting in nonlinear fused-fiber couplers," J. Opt. Soc. Am. B **12**, 898-903 (1995).

10 A. Betlej, S. Suntsov, K. G. Makris, L. Jankovic, D. N. Christodoulides, G. I. Stegeman, J. Fini, R. T. Bise, and D. J. DiGiovanni, "All-optical switching and multifrequency generation in a dual-core photonic crystal fiber," Opt. Lett. **31**, 1480-1482 (2006).

11 K. R. Khan, T. X. Wu, D. N. Christodoulides, and G. I. Stegeman, "Soliton switching and multi-frequency generation in a nonlinear photonic crystal fiber coupler," Opt. Express **16**, 9417-9428 (2008).

investigated through the expressions of the time-dependent nonlinear phase shift in each NLDFC core. The maximum nonlinear phase shifts, ϕ_{max1} and ϕ_{max2}, are related with the spectrum of an optical pulse in the launch and unlaunch NLDFC core, respectively. In this regard, if an optical pulse is propagating through the launch NLDFC core, its spectral content can be obtained by taking the Fourier transform of Eq. (4.6). On the other hand, if an optical pulse is propagating through the unlaunch NLDFC core, its spectral content can be obtained by taking the Fourier transform of Eq. (4.7). In general, the pulse spectrum at the output of each NLDFC core can be obtained by

$$S_m(L,\omega) = \left| \int_{-\infty}^{\infty} U_m(L,T) \exp[i(\omega - \omega_0)T] dT \right|^2 . \qquad (6.1)$$

Figures 6.1 shows the symmetric pulse spectra, of initially unchirped Gaussian pulses, at the output of each NLDFC core for three input values of P_0. Each pulse spectra is normalized and corresponds to a particular separation between both NLDFC cores. As one may expect, the effect of linear coupling reduces the pulse spectra just when the first maximum transfer of optical power is carried out between both NLDFC cores. This is so because the maximum nonlinear phase shift, $\phi_{max1} / \phi_{max1}^{\kappa \to 0}$, is reduced when that first coherent interaction between both NLDFC cores results in an exchange of energy for the first time (see Fig. 4.2). This result can be alternatively seen if we consider the characteristic of the oscillatory structure that covers the entire frequency range of each spectrum. In this sense, the spectral width is reduced by a factor of 1/4 of the number of peaks when an interchange of energy between both NLDFC cores begins.

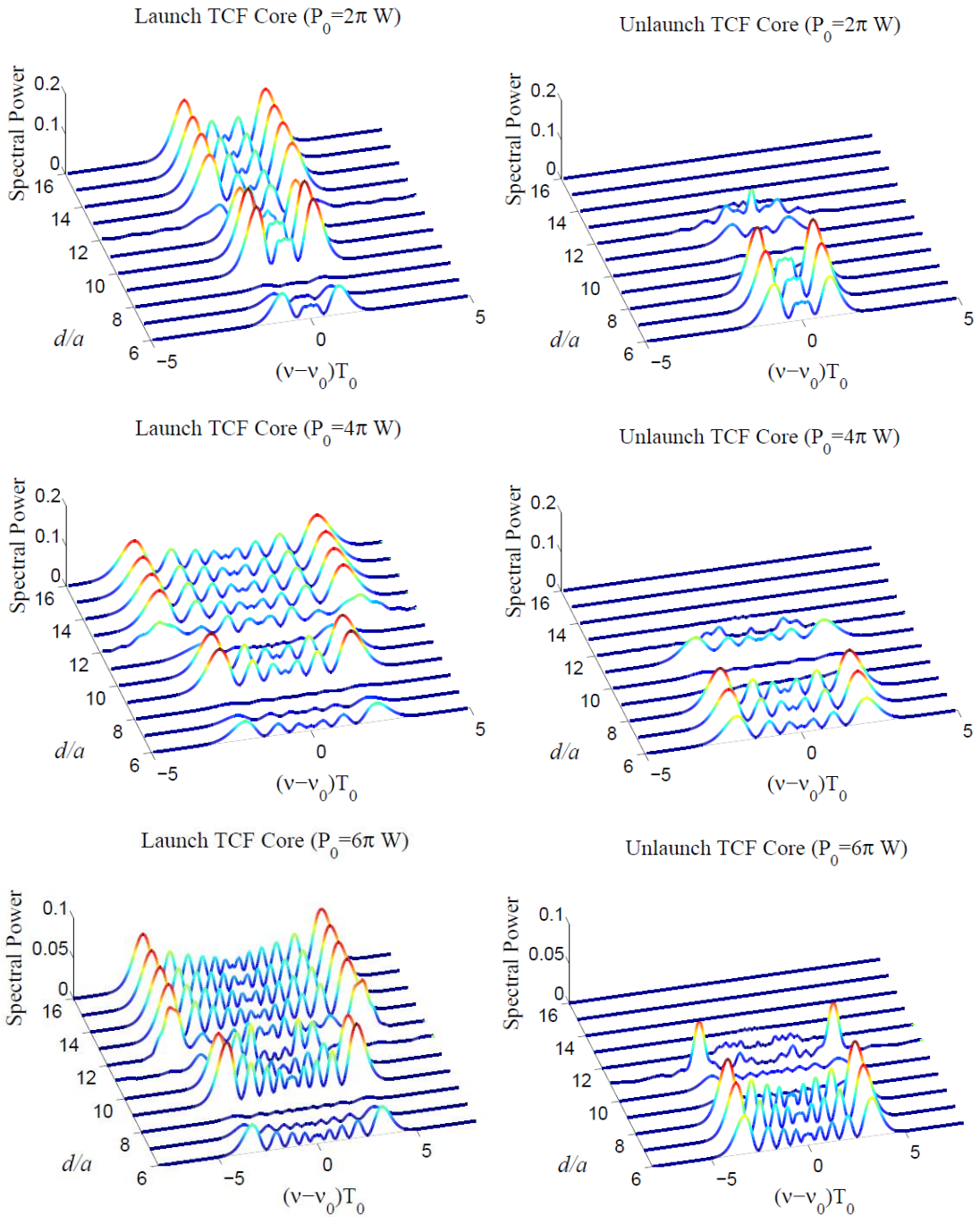

Fig. 6.1 SPM-broadened pulse spectra at the output of the launch and unlaunch NLDFC core for $P_0 = 2\pi$, 4π, and 6π W. Each normalized pulse spectra corresponds to a particular separation between both NLDFC cores.

The number of peaks M and maximum nonlinear phase shift ϕ_{max} before and after the interaction of both NLDFC cores satisfy the standard relation $\phi_{max} = (M\text{-}1/2)\pi$ given in Ref. [1]. In Fig. 6.1 the top, middle, and bottom row shows a reduction of one peak, two peaks and three peaks, respectively.

Although the general case of an input picosecond pulse of arbitrary shape and chirp is applicable to our developed theory, the analysis of an unchirped Gaussian input pulse was suffice and useful to obtain considerable and comprehensive results about the effect of linear coupling on the phenomenon of SPM in NLDFCs. For the case of a chirped Gaussian input pulse, the effect of the initial chirp leads to structural changes in the SPM-broadened pulse spectrum such as in SCFs, however, the performance of the NLDFC is comparable with the case of an unchirped Gaussian input pulse and not much is gained on the spectral narrowing.

Strictly speaking, in the case of considering an asymmetric NLDFC, the linear coupling and mode propagation constant must be different for each NLDFC core. In this regard, the pulse energy is never maximally exchanged from one NLDFC core to the other for the first time and the total suppression of maximum nonlinear phase shift can be smaller than the total suppression when we consider symmetric NLDFC s. Therefore, a NLDFC with dissimilar cores can induces smaller spectral narrowing than a symmetric NLDFC.

To calculate the amount of spectral narrowing induced by the linear coupling, we use the relation of the rms frequency width of a Gaussian input pulse after undergoing SPM. This relation is given by

$$\Delta\omega = \Delta\omega_0 \left(1 + \frac{4}{3\sqrt{3}} \phi_{max}^2 \right)^{1/2}. \tag{6.2}$$

where $\Delta\omega_0$ is the input rms frequency width.

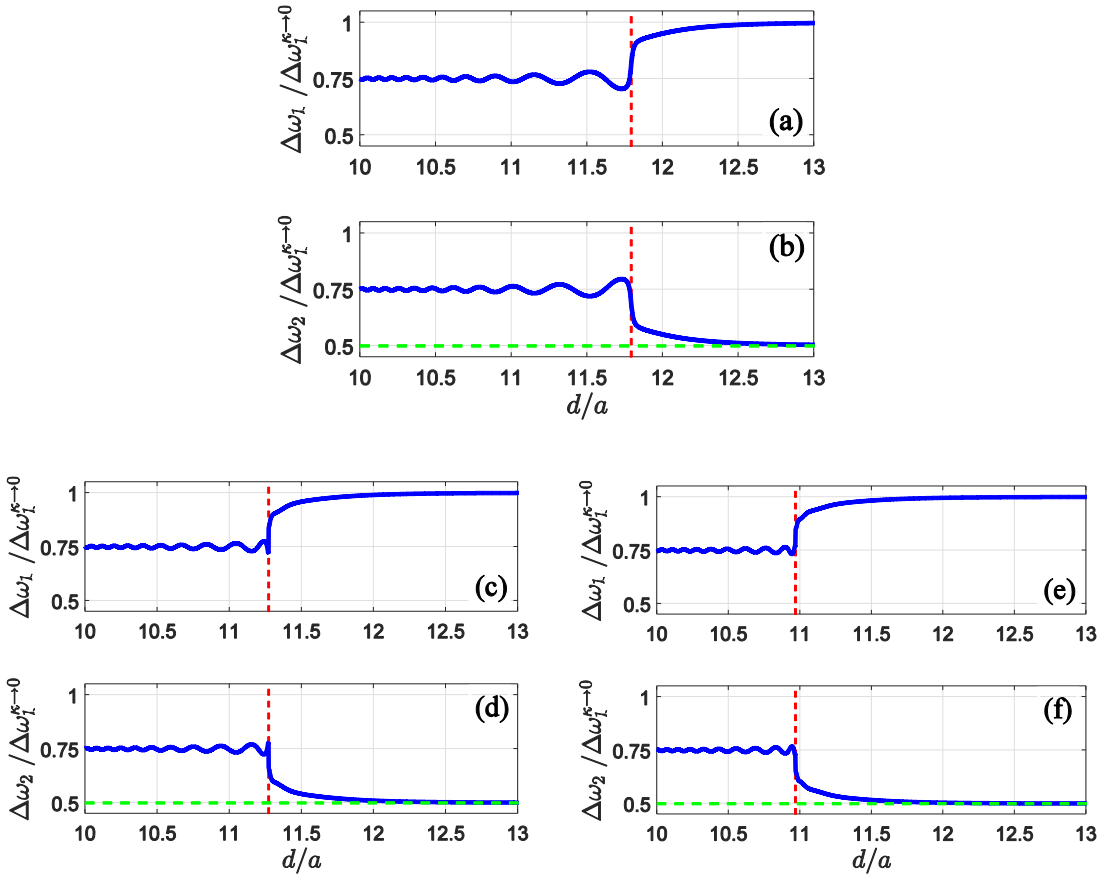

Fig. 6.2 Reduction of the SPM-broadened spectra of a unchirped Gaussian pulse due to linear coupling. (a) and (b) $P_0 = 2\pi$ W, (c) and (d) $P_0 = 4\pi$ W, and (e) and (f) $P_0 = 6\pi$ W. The d/a value related with the κ_c value has been marked down by a red dashed line that separates both NLDFC regimes for each curve.

Figure 6.2 shows the normalized frequency widths, $\Delta\omega_1/\Delta\omega_1^{\kappa\to 0}$ and $\Delta\omega_2/\Delta\omega_1^{\kappa\to 0}$, as a function of d/a for $P_0 = 2\pi, 4\pi$ and 6π W. Here $\Delta\omega_1$ and $\Delta\omega_2$ represent the frequency width of an optical pulse when it is collected at the output of the launch and unlaunch NLDFC core, respectively. The constant limiting value $\Delta\omega_1^{\kappa\to 0}$ represents the frequency width with maximum nonlinear phase shift $\phi_{max1}^{\kappa\to 0} = L/L_{NL}$. The green dashed line represents the limit value for which $\Delta\omega_2/\Delta\omega_1^{\kappa\to 0}$ has not physical interpretation because there is not light in the unlaunch NLDFC core. In fact, we also need to specify that in the Linear Regime some discrete values of $\Delta\omega_1/\Delta\omega_1^{\kappa\to 0}$ and $\Delta\omega_2/\Delta\omega_1^{\kappa\to 0}$ also have not physical interpretation because for those values there is not light in the launch and unlaunch NLDFC core, respectively. We can see how the d/a value related with the κ_c value displaces to the left when P_0 is larger. This same effect can be observed for larger values of γ. In Fig. 6.2, it is clear to see that the amount of spectral narrowing induced by the linear coupling in a NLDFC is one-quarter of the SPM-broadened spectra $\Delta\omega_1^{\kappa\to 0}$. In general, the SPM-broadened spectra of an optical pulse is reduced a quantity that depends on L, P_0, and γ, just when the energy is maximally exchanged from the launch to the unlaunch NLDFC core for the first time. However, the total suppression of frequency width with respect to the $\Delta\omega_1^{\kappa\to 0}$ value is always a constant.

In summary, we conclude that linear coupling induces narrowing in the SPM-broadened spectra of an optical pulse propagating through a NLDFC, just when the first maximum transfer of optical power is carried out between

both NLDFC cores. This is so because the maximum nonlinear phase shift is reduced when that first coherent interaction between both NLDFC cores results in an exchange of energy for the first time. The amount of spectral narrowing induced by linear coupling depend on the peak power of the input optical pulse. We describe this result as an overcoming of linear coupling on SPM effect. In addition, we show that exist a power-dependent critical coupling coefficient that plays a crucial role in the design of NLDFCs.

References

[1] G. P. Agrawal, *Applications of Nonlinear Fiber Optics* (Academic Press, 2008).

[2] R. R. Alfano, The Supercontinuum Laser Source, 2nd ed. (Springer, 2006).

[3] P. V. Mamyshev, "All-optical data regeneration based on self-phase modulation effect," in Proc. European Conference on Optical Communications (ECOC'98), p. 475-476, 1998.

[4] R. H. Stolen and C. Lin, "Self-phase modulation in silica optical fibers," Phys. Rev. A **17**, 1448-1453 (1978).

[5] G. P. Agrawal, Fiber-Optic Communication Systems, 4th ed. (Wiley, 2010).

[6] W. J. Tomlinson, R. H. Stolen, and C. V. Shank, "Compression of optical pulses chirped by self-phase modulation in fibers," J. Opt. Soc. Am. B **1**, 139-149 (1984).

[7] J. van Howe, G. Zhu, and C. Xu, "Compensation of self-phase modulation in fiber-based chirped-pulse amplification systems," Opt. Lett. **31**, 1756-1758 (2006).

[8] Y. S. Kivshar and M. L. Quiroga-Teixeiro, "Influence of cross-phase modulation on soliton switching in nonlinear optical fibers," Opt. Lett. **18**, 980-982 (1993).

[9] P. L. Chu, Y. S. Kivshar, B. A. Malomed, G.-D. Peng, and M. L. Quiroga-Teixeiro, "Soliton controling, switching, and splitting in nonlinear fused-fiber couplers," J. Opt. Soc. Am. B **12**, 898-903 (1995).

[10] A. Betlej, S. Suntsov, K. G. Makris, L. Jankovic, D. N. Christodoulides, G. I. Stegeman, J. Fini, R. T. Bise, and D. J. DiGiovanni, "All-optical switching and multifrequency generation in a dual-core photonic crystal fiber," Opt. Lett. 31, 1480-1482 (2006).

[11] K. R. Khan, T. X. Wu, D. N. Christodoulides, and G. I. Stegeman, "Soliton switching and multi-frequency generation in a nonlinear photonic crystal fiber coupler," Opt. Express 16, 9417-9428 (2008).

Chapter 7

Conclusion

We have developed, for the first time, a comprehensive theory to describe the nonlinear propagation of picosecond pulses through symmetric NLDFCs. Considering the elementary NLDFC switching process, we have derived an exact analytical expression for the optical power and nonlinear phase shift of a picosecond pulse of arbitrary shape and chirp. Applying our results to a Gaussian input pulse, we have shown how the maximum nonlinear phase shift is affected by the linear coupling. To analyze this result, we have defined a critical coupling coefficient that determines the separation of the NLDFC cores at which the pulse energy is maximally exchanged from one NLDFC core to the other for the first time. We also have shown that the critical coupling coefficient plays an important role in the NLDFC performance and has a dramatic impact on the accumulated nonlinear phase shift, and therefore in the frequency spectrum. We also have demonstrated spectral narrowing in the propagation of an initial unchirped pulse through a NLDFC.

Our results have shown that the linear coupling between both NLDFC cores induces that spectral narrowing just when the first maximum transfer of optical power is carried out between both NLDFC cores. This is so because the maximum nonlinear phase shift is reduced when that first coherent interaction between both NLDFC cores results in an exchange of energy for the first time. The amount of spectral narrowing induced by the linear coupling depends on the peak power of the input pulse. However, the total reduction of frequency width is one-quarter of the SPM-broadened spectra. We describe this result as an overcoming of linear coupling on SPM effect.

We have developed, a comprehensive study of the impact of the linear coupling on SPM and nonlinear phase noise in NLDFCs. For this purpose, we have considered a NLDFC with single-mode identical cores and relative lengths in such way that optical losses were ignored. In particular, for a noisy CW beam optical input, we have shown that the variance of the output nonlinear phase shift undergoes a reduction in its saturation value when the joint effects of the linear and nonlinear couplings cause a quasi-periodic power transfer between the two NLDFC cores. This is a result of overcoming the linear coupling on SPM. We have shown that the power-dependent critical coupling coefficient plays a crucial role in the design of NLDFCs. Also, we have found that the variance of the nonlinear phase shift is reduced in proportion with the magnitude of L, P_0, and γ. However, that reduction is a constant with respect to the variance of the nonlinear phase shift which corresponds to the same electromagnetic field propagating along a SCF that has the same physical properties like one NLDFC core. We also have shown that the NLDFC SNR at the output is maximally improved just when the linear

coupling produce that $L=L_c$, when the optical signal is collected from the unlaunch core, and also at $L=2L_c$, when the optical signal is collected from the launch core. When $L=nL_c$, with n growing, the SNR_1 Penalty and SNR_2 Penalty tend to 0 and hence it is not improved by the linear coupling.

Appendix A

Derivation of the Operator Schrödinger-like Equation

The starting point for the derivation of the operator Schrödinger-like equation (Eq. (3.16)) is to rewrite Eqs. (3.14) and (3.15) decomposing $\tilde{\boldsymbol{E}}$, $\tilde{\boldsymbol{H}}$, $\tilde{\boldsymbol{P}}^{(3)}$, and ∇ into their transverse and longitudinal components as

$$\tilde{\boldsymbol{E}} = \tilde{\boldsymbol{E}}_{\mathrm{T}} + \hat{\mathbf{z}}\tilde{E}_{\mathrm{z}}, \tag{A.1}$$

$$\tilde{\boldsymbol{H}} = \tilde{\boldsymbol{H}}_{\mathrm{T}} + \hat{\mathbf{z}}\tilde{H}_{\mathrm{z}}, \tag{A.2}$$

$$\tilde{\boldsymbol{P}}^{(3)} = \tilde{\boldsymbol{P}}_{\mathrm{T}}^{(3)} + \hat{\mathbf{z}}\tilde{P}_{\mathrm{z}}^{(3)}, \tag{A.3}$$

$$\nabla = \nabla_{\mathrm{T}} + \hat{\mathbf{z}}\partial_{\mathrm{z}}. \tag{A.4}$$

Therefore, Eqs. (3.14) and (3.15) become

$$\begin{aligned}\nabla_T\times(\nabla_T\times\tilde{\boldsymbol{E}}_T)+\hat{\mathbf{z}}\partial_z\times(\nabla_T\times\tilde{\boldsymbol{E}}_T)+\nabla_T\times[\nabla_T\times(\hat{\mathbf{z}}\tilde{E}_z)]\\ +\hat{\mathbf{z}}\partial_z\times[\nabla_T\times(\hat{\mathbf{z}}\tilde{E}_z)]+\nabla_T\times[\partial_z(\hat{\mathbf{z}}\times\tilde{\boldsymbol{E}}_T)]\\ +\hat{\mathbf{z}}\partial_z\times[\partial_z(\hat{\mathbf{z}}\times\tilde{\boldsymbol{E}}_T)]-n^2k_0^2\tilde{\boldsymbol{E}}_T-\hat{\mathbf{z}}n^2k_0^2\tilde{E}_z\\ =\omega^2\mu_0\tilde{\boldsymbol{P}}_T^{(3)}+\hat{\mathbf{z}}\omega^2\mu_0\tilde{P}_z^{(3)},\end{aligned}\tag{A.5}$$

$$\begin{aligned}\nabla_T\times\frac{1}{n^2}(\nabla_T\times\tilde{\boldsymbol{H}}_T)+\hat{\mathbf{z}}\partial_z\times\frac{1}{n^2}(\nabla_T\times\tilde{\boldsymbol{H}}_T)+\nabla_T\times\frac{1}{n^2}[\nabla_T\times(\hat{\mathbf{z}}\tilde{H}_z)]\\ +\hat{\mathbf{z}}\partial_z\times\frac{1}{n^2}[\nabla_T\times(\hat{\mathbf{z}}\tilde{H}_z)]+\nabla_T\times\frac{1}{n^2}[\partial_z(\hat{\mathbf{z}}\times\tilde{\boldsymbol{H}}_T)]\\ +\hat{\mathbf{z}}\partial_z\times\frac{1}{n^2}[\partial_z(\hat{\mathbf{z}}\times\tilde{\boldsymbol{H}}_T)]-k_0^2\tilde{\boldsymbol{H}}_T-\hat{\mathbf{z}}k_0^2\tilde{H}_z\\ =-\hat{\mathbf{z}}i\omega\partial_z\times\hat{\mathbf{z}}\frac{1}{n^2}\tilde{P}_z^{(3)}-i\omega\nabla_T\times\frac{1}{n^2}\tilde{\boldsymbol{P}}_T^{(3)}\\ -\hat{\mathbf{z}}i\omega\partial_z\times\frac{1}{n^2}\tilde{\boldsymbol{P}}_T^{(3)}-i\omega\nabla_T\times\hat{\mathbf{z}}\frac{1}{n^2}\tilde{P}_z^{(3)},\end{aligned}\tag{A.6}$$

where $\hat{\mathbf{z}}\partial_z\times\hat{\mathbf{z}}\tilde{E}_z=0$ and $\hat{\mathbf{z}}\partial_z\times\hat{\mathbf{z}}\tilde{H}_z=0.$

Applying the Fourier transform to the time-dependent Maxwell´s equations (Eqs. (3.1) and (3.2)), and using the relations given by Eqs. (A.1)-(A.4), we obtain

$$\nabla_T\times\tilde{\boldsymbol{E}}_T+\nabla_T\times(\hat{\mathbf{z}}\tilde{E}_z)+\partial_z(\hat{\mathbf{z}}\times\tilde{\boldsymbol{E}}_T)=i\omega\mu_0\tilde{\boldsymbol{H}}_T+\hat{\mathbf{z}}i\omega\mu_0\tilde{H}_z,\tag{A.7}$$

$$\begin{aligned}\nabla_T\times\tilde{\boldsymbol{H}}_T+\nabla_T\times(\hat{\mathbf{z}}\tilde{H}_z)+\partial_z(\hat{\mathbf{z}}\times\tilde{\boldsymbol{H}}_T)=\\ -i\omega\varepsilon_0n^2\tilde{\boldsymbol{E}}_T-\hat{\mathbf{z}}i\omega\varepsilon_0n^2\tilde{E}_z-i\omega\tilde{\boldsymbol{P}}_T^{(3)}-\hat{\mathbf{z}}i\omega\tilde{P}_z^{(3)},\end{aligned}\tag{A.8}$$

where $\tilde{\boldsymbol{P}} = \tilde{\boldsymbol{P}}^{L} + \tilde{\boldsymbol{P}}^{NL} = \varepsilon_0(n^2 - 1)\tilde{\boldsymbol{E}} + \tilde{\boldsymbol{P}}^{(3)}$. Identifying the transverse and longitudinal terms of Eqs. (A.7) and (A.8), we obtain

$$\nabla_T \times (\hat{\mathbf{z}}\tilde{E}_z) + \partial_z(\hat{\mathbf{z}} \times \tilde{\boldsymbol{E}}_T) = i\omega\mu_0 \tilde{\boldsymbol{H}}_T, \tag{A.9}$$

$$\nabla_T \times \tilde{\boldsymbol{E}}_T = \hat{\mathbf{z}} i\omega\mu_0 \tilde{H}_z, \tag{A.10}$$

$$\nabla_T \times (\hat{\mathbf{z}}\tilde{H}_z) + \partial_z(\hat{\mathbf{z}} \times \tilde{\boldsymbol{H}}_T) = -i\omega\varepsilon_0 n^2 \tilde{\boldsymbol{E}}_T - i\omega\tilde{\boldsymbol{P}}_T^{(3)}, \tag{A.11}$$

$$\nabla_T \times \tilde{\boldsymbol{H}}_T = -\hat{\mathbf{z}} i\omega\varepsilon_0 n^2 \tilde{E}_z - \hat{\mathbf{z}} i\omega \tilde{P}_z^{(3)}. \tag{A.12}$$

Multiplying Eq. (A.9) by $\nabla_T \times$, Eq. (A.10) by $-i\omega\varepsilon_0$, Eq. (A.11) by $\nabla_T \times \frac{1}{n^2}$, and Eq. (A.12) by $i\omega\mu_0$, we obtain

$$\nabla_T \times \nabla_T \times (\hat{\mathbf{z}}\tilde{E}_z) + \nabla_T \times \partial_z(\hat{\mathbf{z}} \times \tilde{\boldsymbol{E}}_T) = i\omega\mu_0(\nabla_T \times \tilde{\boldsymbol{H}}_T), \tag{A.13}$$

$$-i\omega\varepsilon_0(\nabla_T \times \tilde{\boldsymbol{E}}_T) = \hat{\mathbf{z}} k_0^2 \tilde{H}_z, \tag{A.14}$$

$$\begin{aligned} \nabla_T \times \frac{1}{n^2} \nabla_T \times (\hat{\mathbf{z}}\tilde{H}_z) + \nabla_T \times \frac{1}{n^2} \partial_z(\hat{\mathbf{z}} \times \tilde{\boldsymbol{H}}_T) \\ = -i\omega\varepsilon_0(\nabla_T \times \tilde{\boldsymbol{E}}_T) - i\omega \nabla_T \times \frac{1}{n^2} \tilde{\boldsymbol{P}}_T^{(3)}, \end{aligned} \tag{A.15}$$

$$i\omega\mu_0(\nabla_T \times \tilde{\boldsymbol{H}}_T) = \hat{\mathbf{z}} k_0^2 n^2 \tilde{E}_z + \hat{\mathbf{z}}\mu_0\omega^2 \tilde{P}_z^{(3)}. \tag{A.16}$$

Substituting Eq. (A.16) into Eq. (A.13), and Eq. (A.14) into Eq. (A.15), we obtain

$$\nabla_T \times \nabla_T \times (\hat{\mathbf{z}}\tilde{E}_z) + \nabla_T \times \partial_z(\hat{\mathbf{z}} \times \tilde{\boldsymbol{E}}_T) = \hat{\mathbf{z}} k_0^2 n^2 \tilde{E}_z + \hat{\mathbf{z}}\mu_0\omega^2 \tilde{P}_z^{(3)}, \tag{A.17}$$

$$\nabla_T \times \frac{1}{n^2}\nabla_T \times (\hat{\mathbf{z}}\tilde{H}_z) + \nabla_T \times \frac{1}{n^2}\partial_z(\hat{\mathbf{z}} \times \tilde{\boldsymbol{H}}_T) = \hat{\mathbf{z}}k_0^2\tilde{H}_z - i\omega\nabla_T \times \frac{1}{n^2}\tilde{\boldsymbol{P}}_T^{(3)}. \quad \text{(A.18)}$$

Using Eqs. (A.17) and (A.18), we can rewrite Eqs. (A.5) and (A.6) as

$$\nabla_T \times (\nabla_T \times \tilde{\boldsymbol{E}}_T) + i\omega\mu_0\partial_z(\hat{\mathbf{z}} \times \tilde{\boldsymbol{H}}_T) - n^2k_0^2\tilde{\boldsymbol{E}}_T = \omega^2\mu_0\tilde{\boldsymbol{P}}_T^{(3)}, \quad \text{(A.19)}$$

$$\nabla_T \times \frac{1}{n^2}(\nabla_T \times \tilde{\boldsymbol{H}}_T) - i\omega\varepsilon_0\partial_z(\hat{\mathbf{z}} \times \tilde{\boldsymbol{E}}_T) - k_0^2\tilde{\boldsymbol{H}}_T = -i\omega\nabla_T \times \hat{\mathbf{z}}\frac{1}{n^2}\tilde{P}_z^{(3)}. \quad \text{(A.20)}$$

where $\hat{\mathbf{z}}\partial_z \times [\nabla_T \times (\hat{\mathbf{z}}\tilde{E}_z)] + \hat{\mathbf{z}}\partial_z \times [\partial_z(\hat{\mathbf{z}} \times \tilde{\boldsymbol{E}}_T)] = i\omega\mu_0\partial_z\hat{\mathbf{z}} \times \tilde{\boldsymbol{H}}_T$, $\hat{\mathbf{z}}\partial_z \times \frac{1}{n^2}\nabla_T \times (\hat{\mathbf{z}}\tilde{H}_z)$ $+\hat{\mathbf{z}}\partial_z \times \frac{1}{n^2}\partial_z(\hat{\mathbf{z}} \times \tilde{\boldsymbol{H}}_T) = -i\omega\varepsilon_0\partial_z\hat{\mathbf{z}} \times \tilde{\boldsymbol{E}}_T - i\omega\partial_z\hat{\mathbf{z}} \times \frac{1}{n^2}\tilde{\boldsymbol{P}}_T^{(3)}$, $\hat{\mathbf{z}}\partial_z \times \frac{1}{n^2}\partial_z\hat{\mathbf{z}} \times \tilde{\boldsymbol{H}}_T = 0$, and $\hat{\mathbf{z}}\partial_z \times (\nabla_T \times \tilde{\boldsymbol{E}}_T) = 0$.